SUPPORTING INFORMATION

Synthetic, structural, NMR and catalytic study of phosphinic amide-phosphoryl chalcogenides (chalcogen = O, S, Se) as mixed-donor bidentate ligands in zinc chemistry

Miguel A. del Águila-Sánchez,[a] Neidemar M. Santos-Bastos,[b] Maria C. Ramalho-Freitas,[c] Jesús García López,[a] Marcos Costa de Souza,[b] Jackson A. L. Camargos-Resende,[c] María Casimiro,[a] Gilberto Alves-Romeiro,[b] María José Iglesias[a] and Fernando López Ortiz*[a]

[a]*Área de Química Orgánica, Universidad de Almería, Carretera de Sacramento s/n, 04120, Almería, Spain. E-mail: flortiz@ual.es*
[b] *Departamento de Química Orgânica, Universidade Federal Fluminense, Instituto de Química, Rio de Janeiro, Brazil.*
[c]*Departamento de Química Inorgânica, Universidade Federal Fluminense, Instituto de Química, Rio de Janeiro, Brazil.*

Contents

NMR structural assignment of complex 21a

A strategy followed for the NMR structural assignment of **21a** is shown in Table S1. Carbons scalarly coupled to a given phosphorus atom were identified through the ^{13}C NMR spectra measured with selective ^{31}P decoupling of the phosphinic amide nucleus, $^{13}C\{^{1}H,^{31}P_{ON}\}$. Carbons of the ortho disubstituted phenyl ring are coupled to both phosphorus atoms. They could be assigned based on the different magnitude of $^{n}J_{PC}$ (n = 1 >> n = 2 ≈ n = 3 > n = 4) and the correlations observed in the $^{1}H,^{13}C$-gHSQC spectrum. For instance, the collapse of $^{1}J_{PC}$ in the $^{13}C\{^{1}H,^{31}P_{ON}\}$ spectrum furnished the straightforward assignment of C1 (δ 135.89 ppm, dd, $^{1}J_{PC}$ = 127.5, $^{2}J_{PC}$ = 9.5 Hz) and C2 (δ 133.73 ppm, dd, $^{1}J_{PC}$ = 97.9, $^{2}J_{PC}$ = 13.3 Hz). The unequivocal identification of the key protons of this ring H3 and H6 was obtained from 1D gNOESY spectra. Thus, selective inversion of H6 (δ 8.37 ppm) produces positive NOE on H5 (δ 7.91 ppm) and H20/24 (δ 7.28 ppm), the latter being ortho protons of the phenyl ring bound to the phosphinic amide phosphorus. Irradiation of the multiplet at δ 7.18 ppm (2H) induces a small NOE on H20/24, thus identifying the irradiated protons as H14/18, i.e., the ortho protons of the P(O)-phenyl group oriented in the same direction as the NP(O)-phenyl ring. This NOE implies that the seven-membered metallacycle must adopt a distorted conformation that brings closer the phenyl rings of both ortho substituents, most likely to alleviate steric interactions arising from the bulky $N^{i}Pr_2$ moiety. The ortho protons H8/12 of the remaining P(O)-Ph group appear at δ 7.57 ppm, as deduced from the NOE observed upon irradiation of this multiplet with the signals of H14/18 and H3 (δ 7.33 ppm). H3 is the proton most affected by ligand coordination to zinc (see Table S1). It suffers a shielding of 1.25 ppm (average for **21a-c** of ca. 1.1 ppm) that can be assigned to magnetic anisotropy effects. Building up the zinc matallacycle will allocate H3 in the region of the magnetic anisotropy shielding cone of a phenyl ring of the $Ph_2P{=}X$ moiety.

Once assigned the three H_{ortho} signals, they were used as the starting point in the analysis of the COSY45 spectrum to identify all other aromatic protons. In this way, the respective H_{meta} were identified (δ 6.99, m, H21/23; 7.04, m, H15/17; 7.39, m, H9/11 ppm). Their correlations in the HMBC spectrum via $^{3}J_{CH}$ with the corresponding quaternary carbons allowed to assign the C_{ipso} carbons C7 (δ 129.87 ppm, d, $^{1}J_{PC}$ = 115.3 Hz), C13 (δ 126.49 ppm, d, $^{1}J_{PC}$ = 108.1 Hz) and C19 (δ 128.36 ppm, d, $^{1}J_{PC}$ = 126,7 Hz).

Table S1 Selected NMR data of **20a-b** and **21** (δ in ppm and *J* Hz) and schematic representation of the structure assignment of **21a** based on NMR spectra. The numbering scheme used is included. Colored fragments indicate scalar coupling to one (green and rose) or two (blue) ^{31}P nuclei. Plain and dashed arrows indicate, respectively, ^{1}H,^{31}C long-range correlations and nuclear Overhauser enhancements.

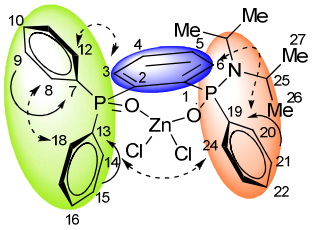

δ/$^{n}J_{PC}$	**20a**	**20b**	**21a**	**21b**	**21c**
C1/ $^{1}J_{PC,}$ $^{2}J_{PC}$	138.01/ 127.6, 9.2	137.51/ 127.5, 9.1	135.89/ 127.5, 9.5	135.24/ 133.4, 9.7	135.38/ 135.1, 9.3
C2/ $^{1}J_{PC,}$ $^{2}J_{PC}$	136.11/ 96.4, 12.0	136.97/ 79.3, 11.1	133.73/ 97.9, 13.3	135.65/ 80.7, 12.7	134.55/ 71.1, 10.9
C3/ $^{2}J_{PC,}$ $^{3}J_{PC}$	137.23/ 9.1, 10.9	137.22/ 13.4, 11.4	137.71/ 11.8, 14.7	138.04/ 11.8, 11.8	137.55/ 12.0, 12.0
C7/ $^{1}J_{PC}$	134.07/ 111.4	135.07/ 90.3	129.87/ 115.3	130.93/ 90.8	130.71/ 80.7
C13/ $^{1}J_{PC}$	134.34/ 111.7	135.70/ 89.9	126.49/ 108.1	124.6/ 86.0	123.23/ 79.1
C19/ $^{1}J_{PC}$	132.86/ 123.4	133.02/ 122.4	128.36/ 126.7	128.96/ 130.9	129.22/ 132.9
H3	8.58	8.18	7.33	7.30	7.23

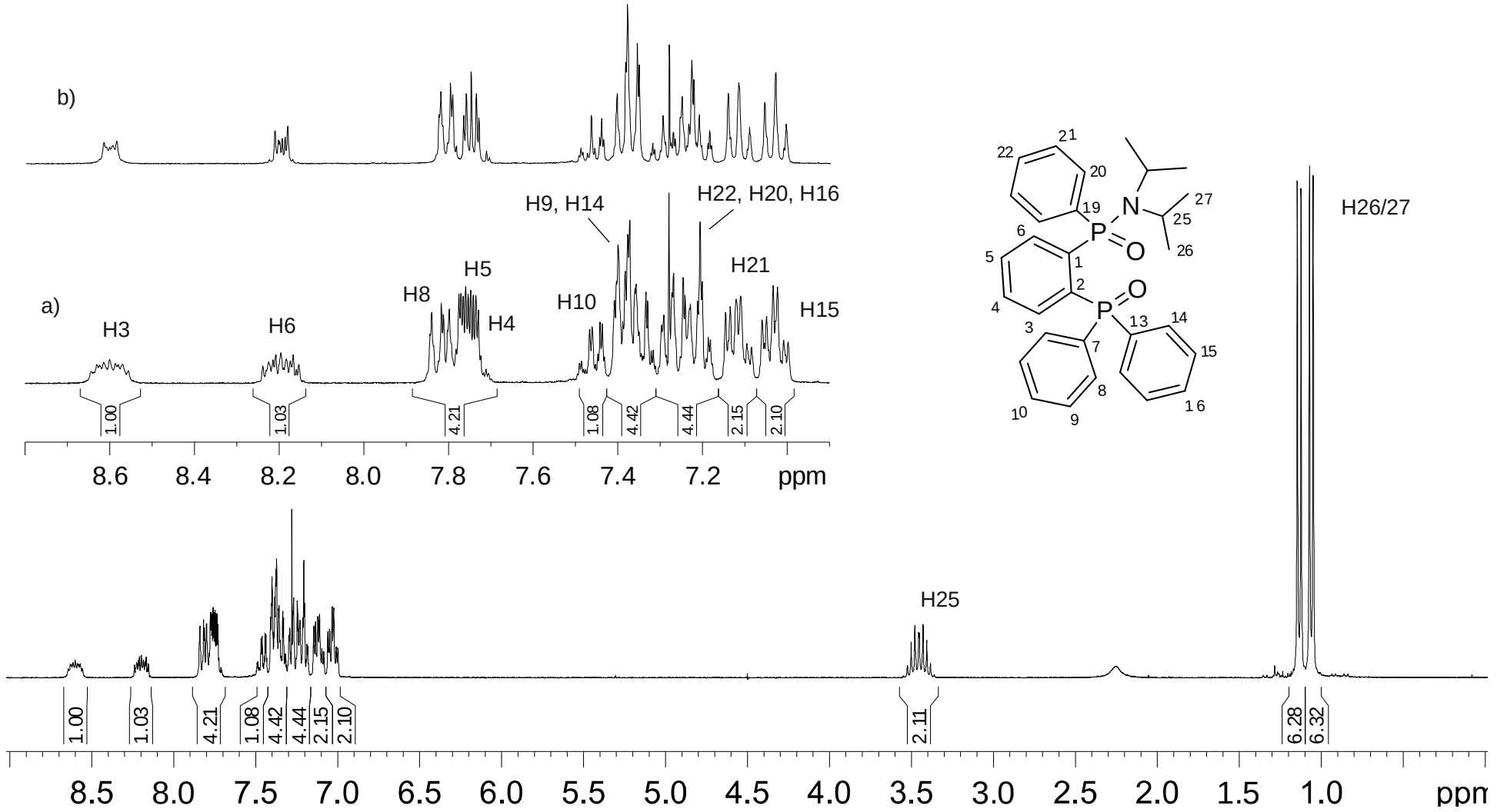

Figure S1. (a) ^{1}H- and (b) ^{1}H $\{^{31}$P$\}$-NMR spectra of ligand **20a.**

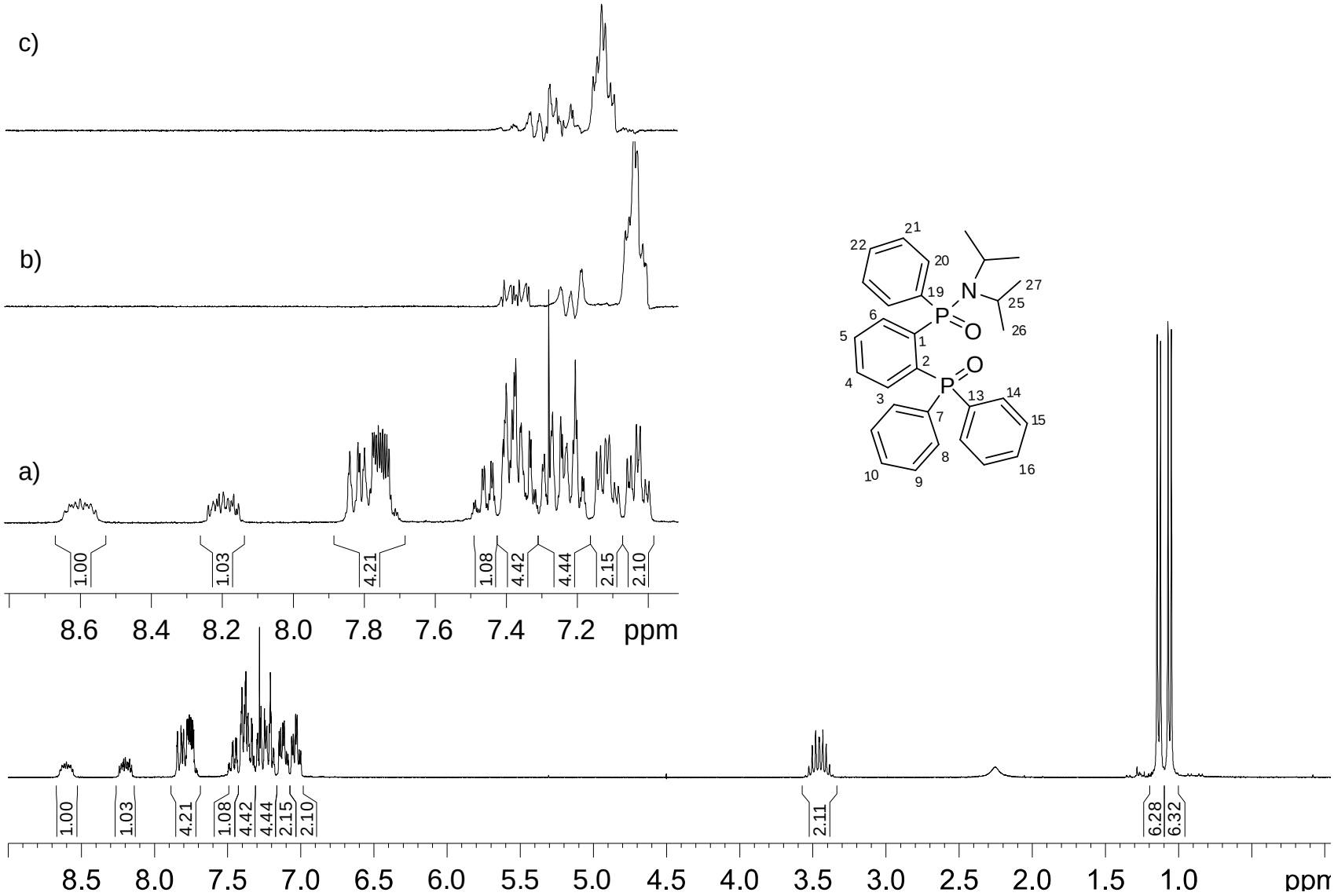

Figure S2. (a) ^{1}H-NMR and (b – c) 1D-TOCSY NMR spectra of ligand **20a** with selective excitation of (b) H15 at δ 7.01 ppm and (c) H21 at δ 7.10 ppm**.**

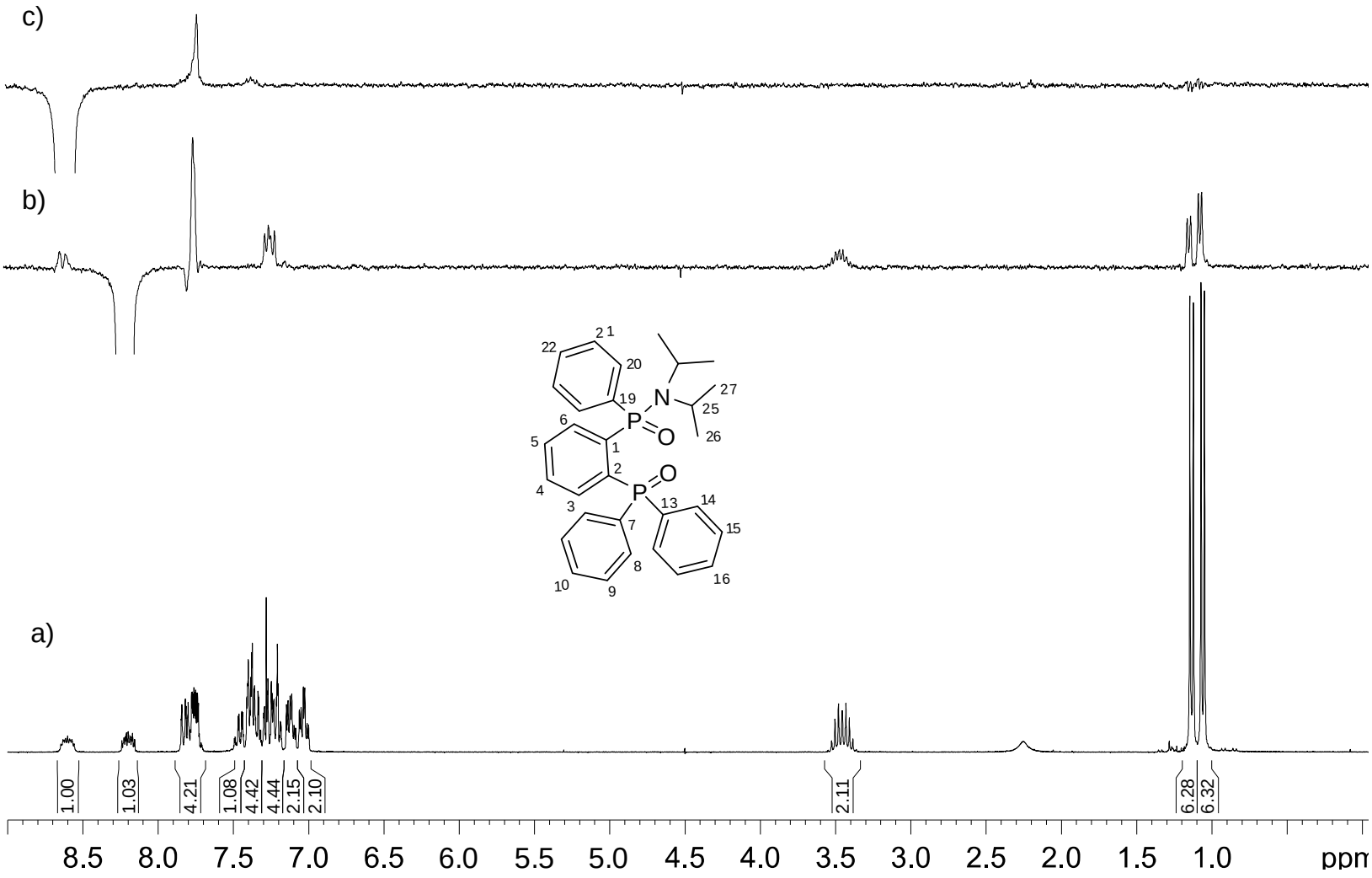

Figure S3. (a) ^{1}H-NMR and (b – c) 1D-NOESY NMR spectra of ligand **20a** with selective inversion at (b) H6 at δ 8.18 ppm and (c) H3 at δ 8.58 ppm)**.**

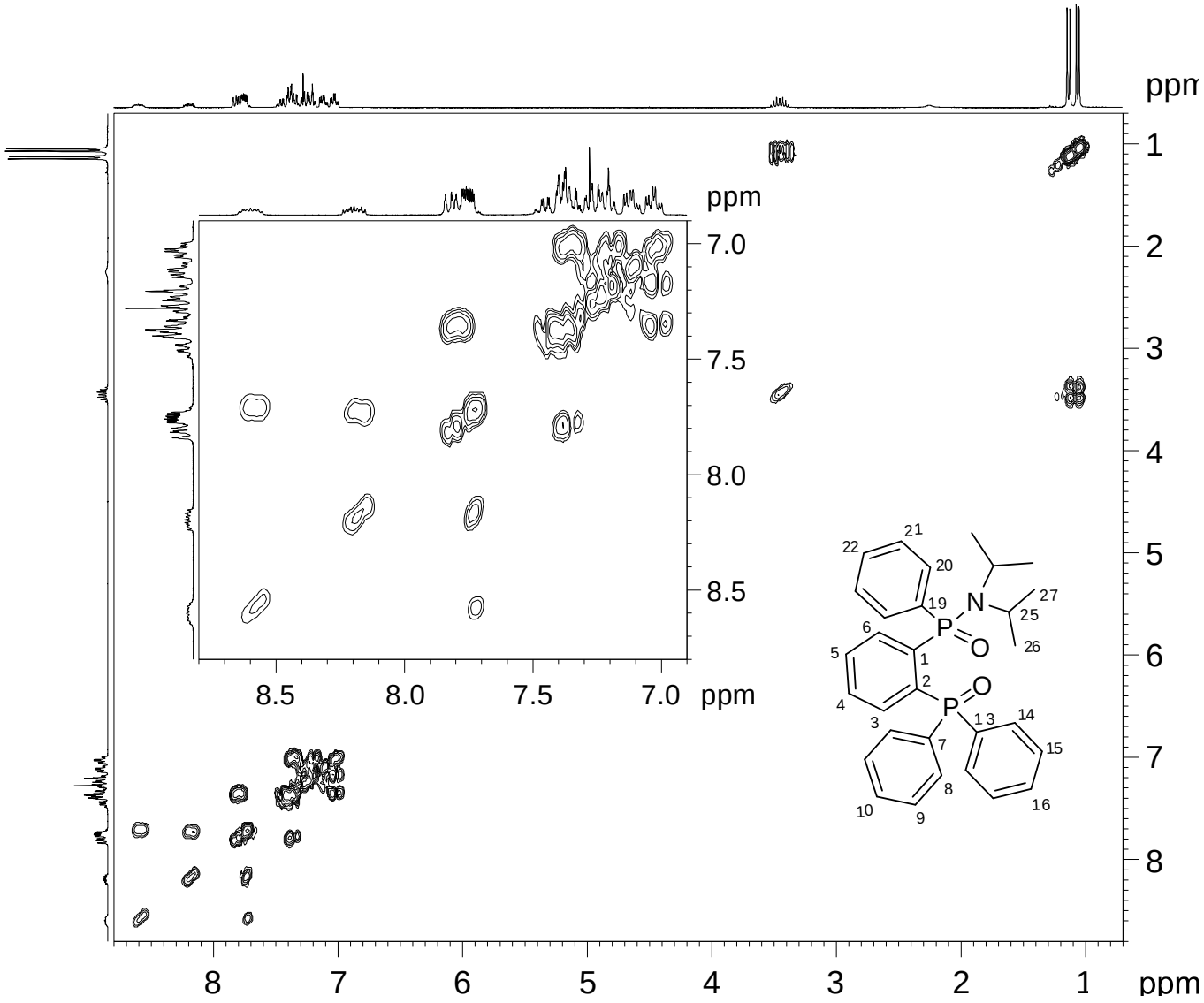

Figure S4. ^{1}H,^{1}H-COSY45 spectrum of ligand **20a** including an expansion of the region of aromatic protons.

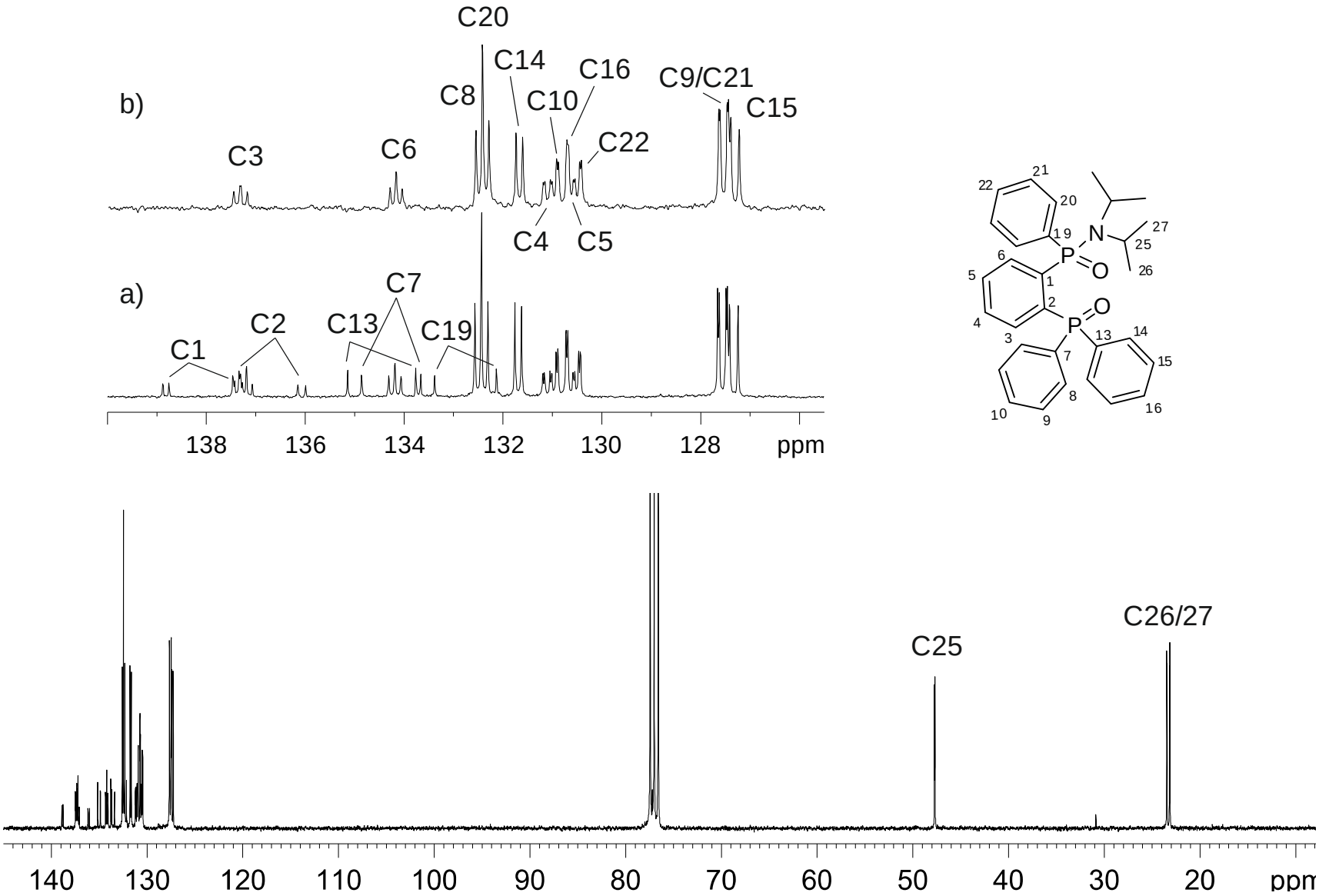

Figure S5. (a) $^{13}C\{^{1}H\}$- and (b) dept135 (aromatic region) NMR spectra of ligand **20a.**

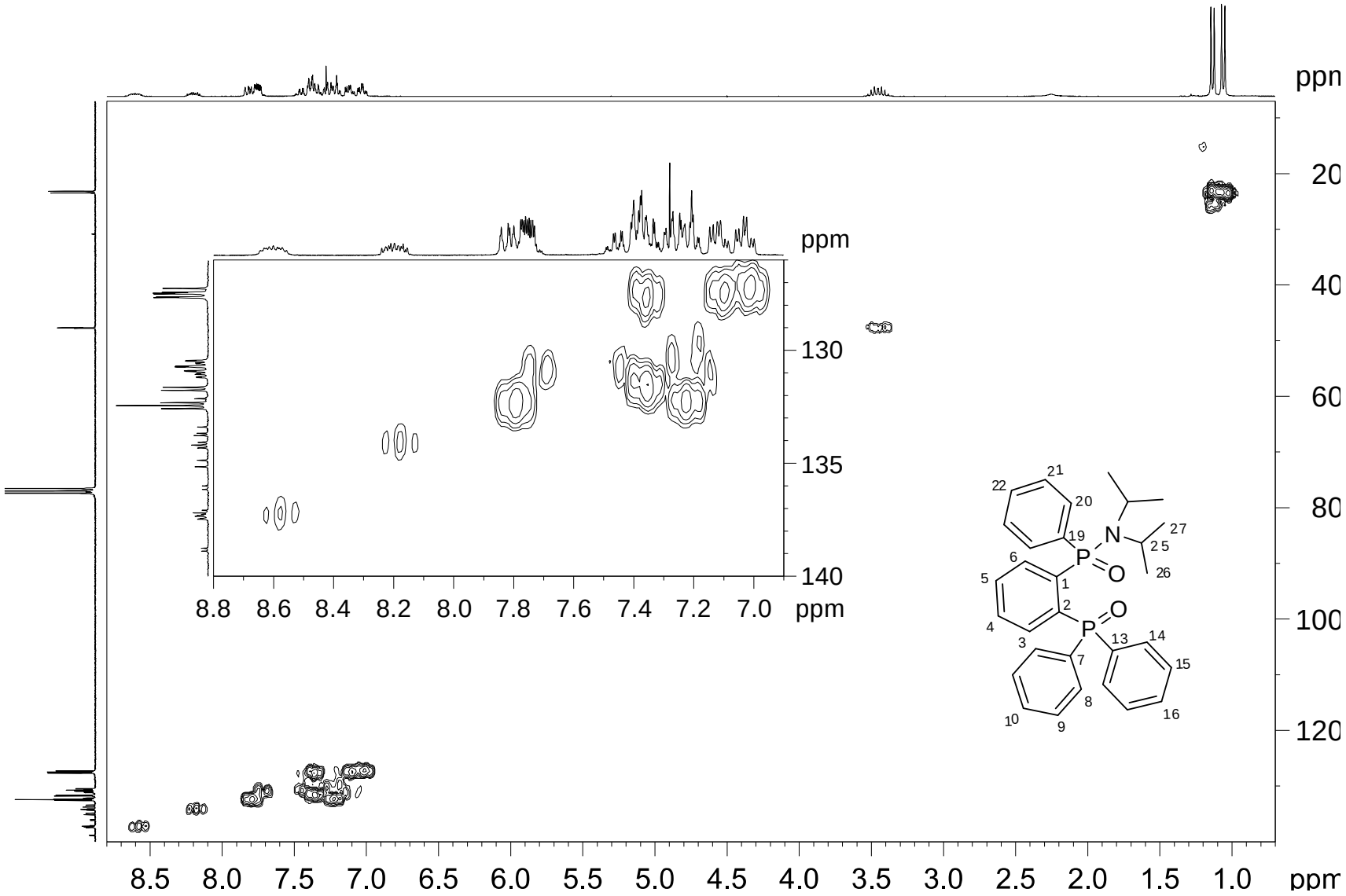

Figure S6. $^{1}H,^{13}C$-HSQC spectrum of ligand **20a** including an expansion of the region ofaromatic protons**.**

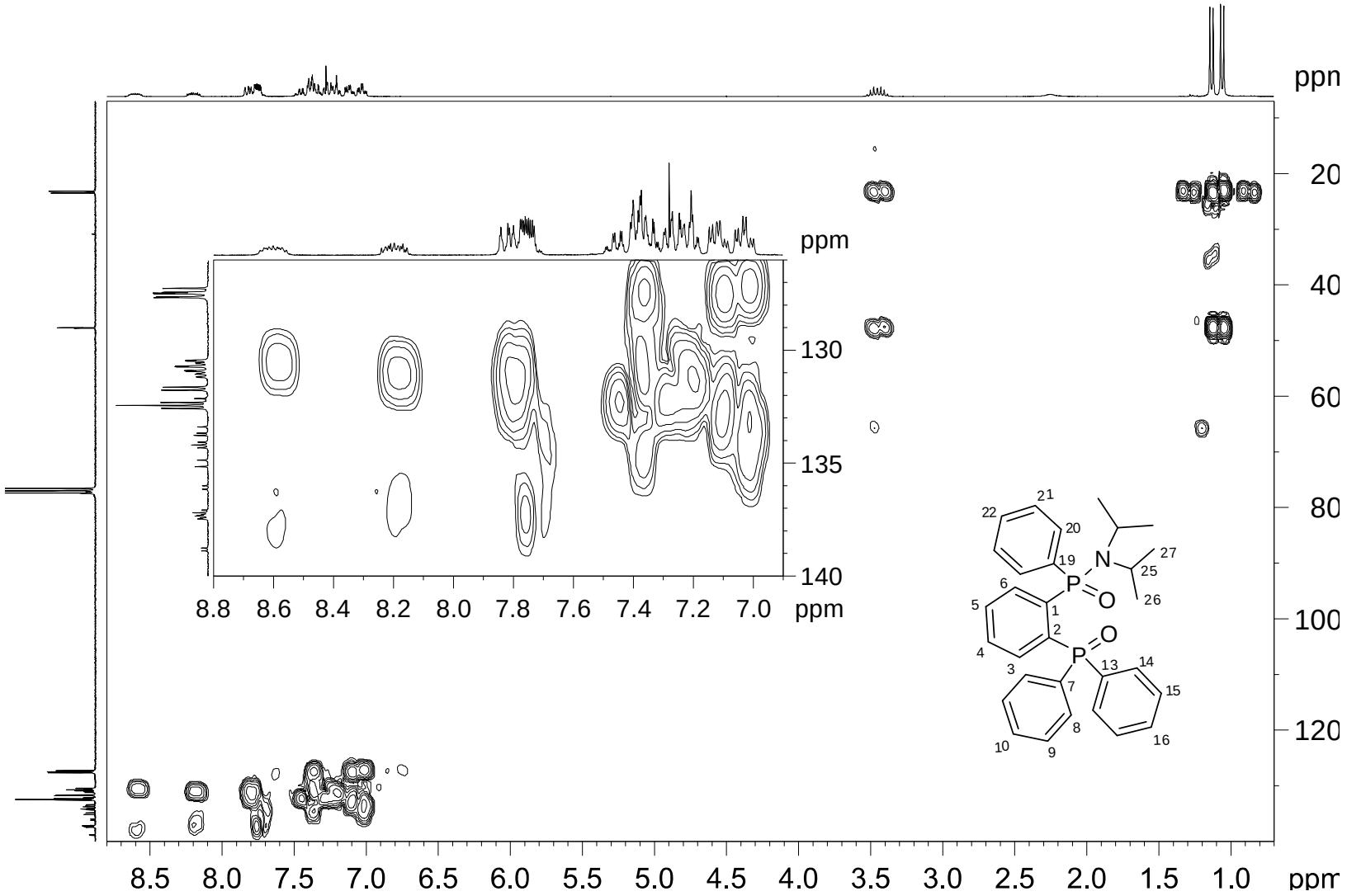

Figure S7. $^{1}H,^{13}C$-HMBC spectrum of ligand **20a** including an expansion of the region of aromatic protons**.**

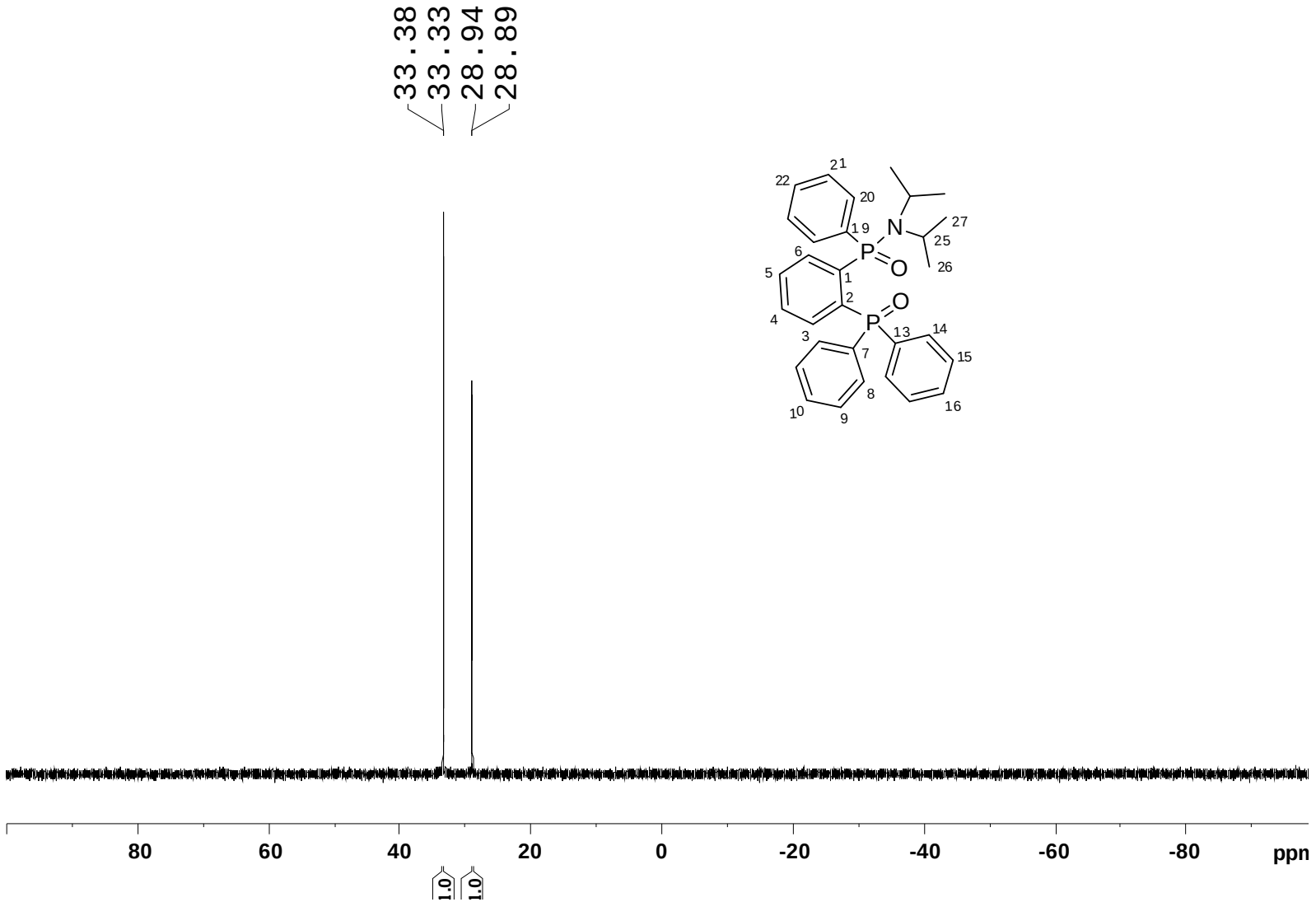

Figure S8. $^{31}P\{^{1}H\}$-NMR spectrum of ligand **20a.**

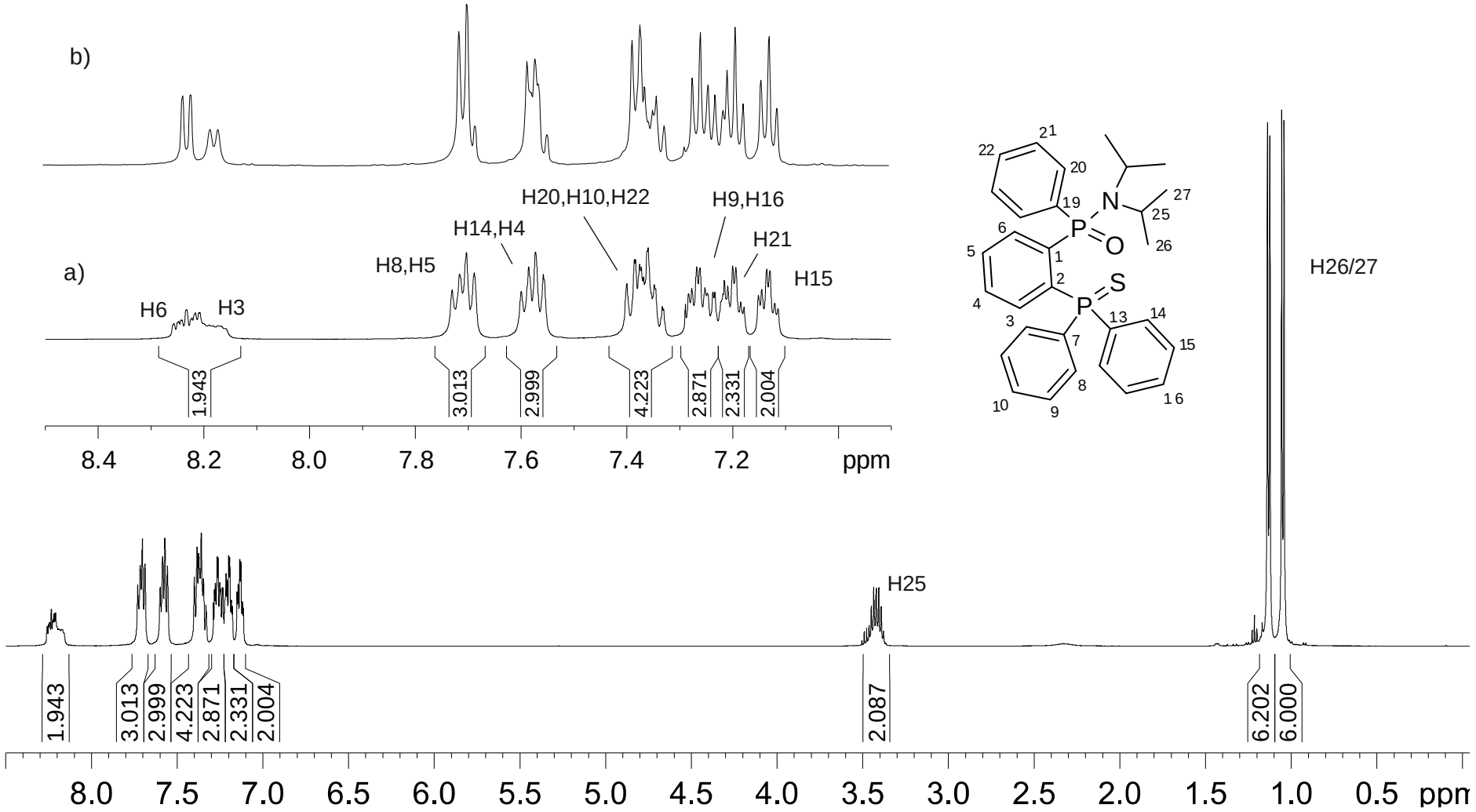

Figure S9. (a) ^{1}H- and (b) ^{1}H $\{^{31}$P$\}$-NMR spectra of ligand **20b.**

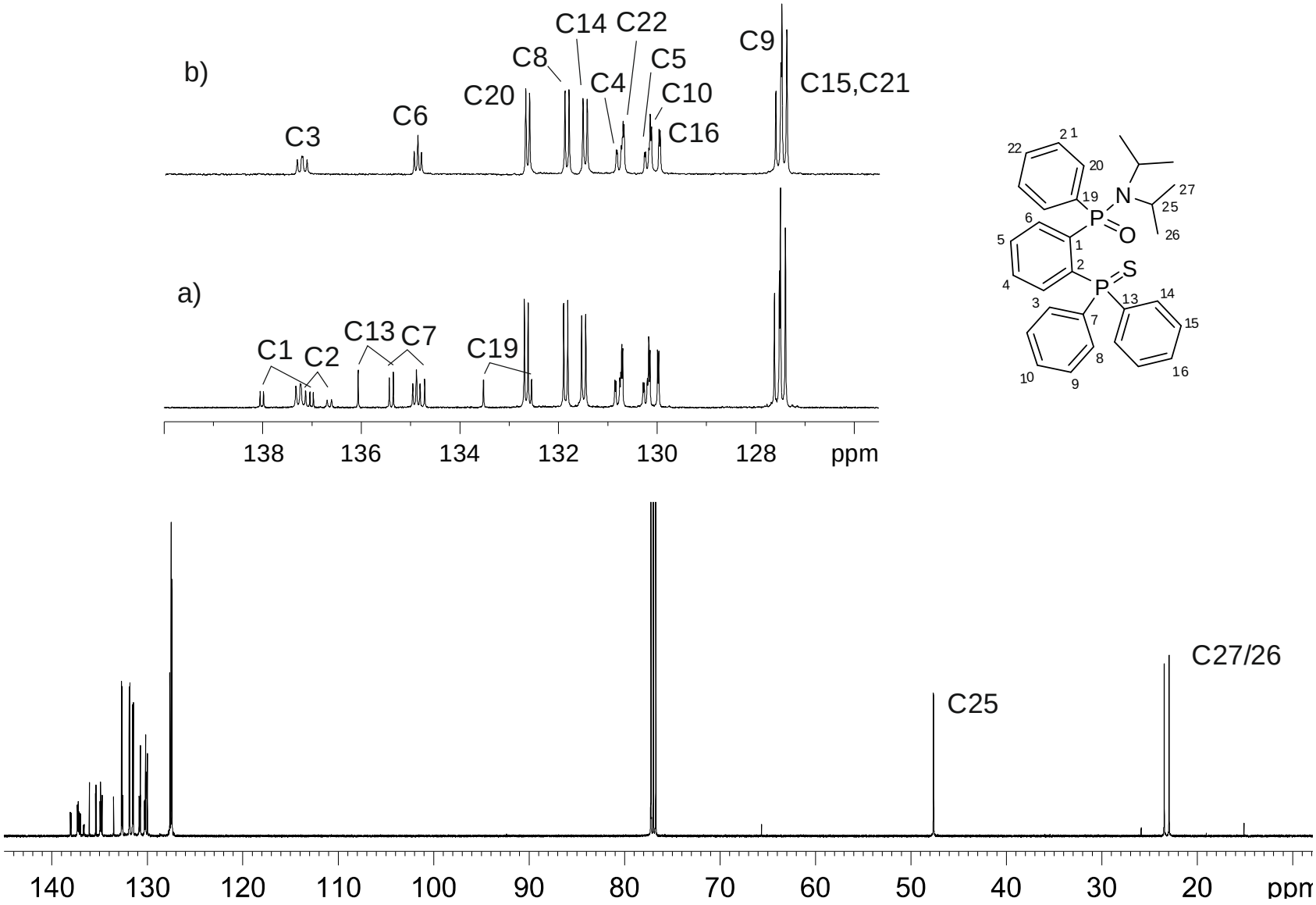

Figure S10. (a) $^{13}C\{^{1}H\}$- and (b) dept135 (aromatic region) NMR spectra of ligand **20b.**

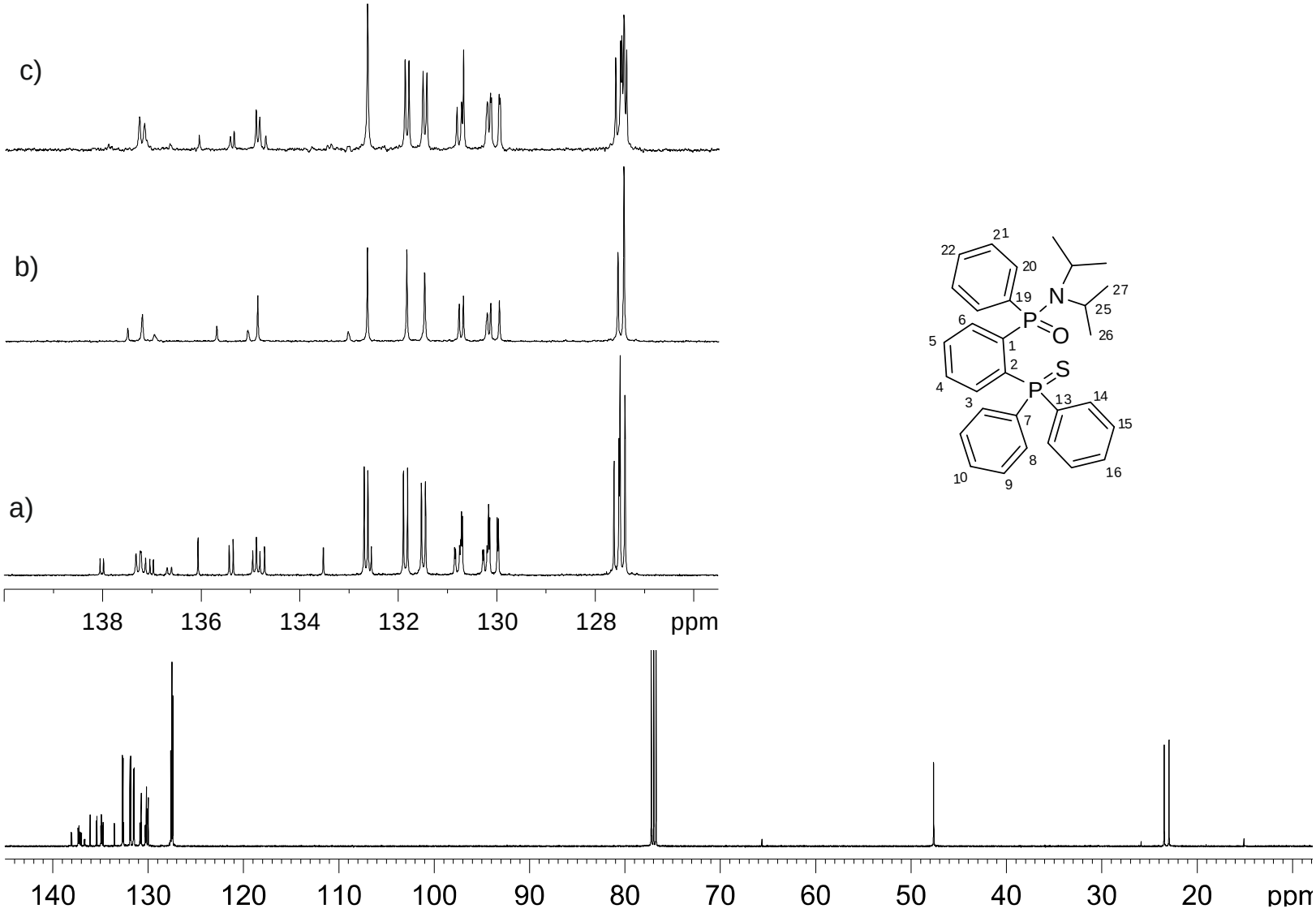

Figure S11. (a) $^{13}C\{^{1}H\}$-, (b) $^{13}C\{^{1}H, ^{31}P\}$- and (c) $^{13}C\{^{1}H, ^{31}P_{P=O}\}$- (selective decoupling of the ^{31}P signal at δ 28.11 ppm) NMR spectra of ligand **20b**. In (b) and (c) only the aromatic region is shown.

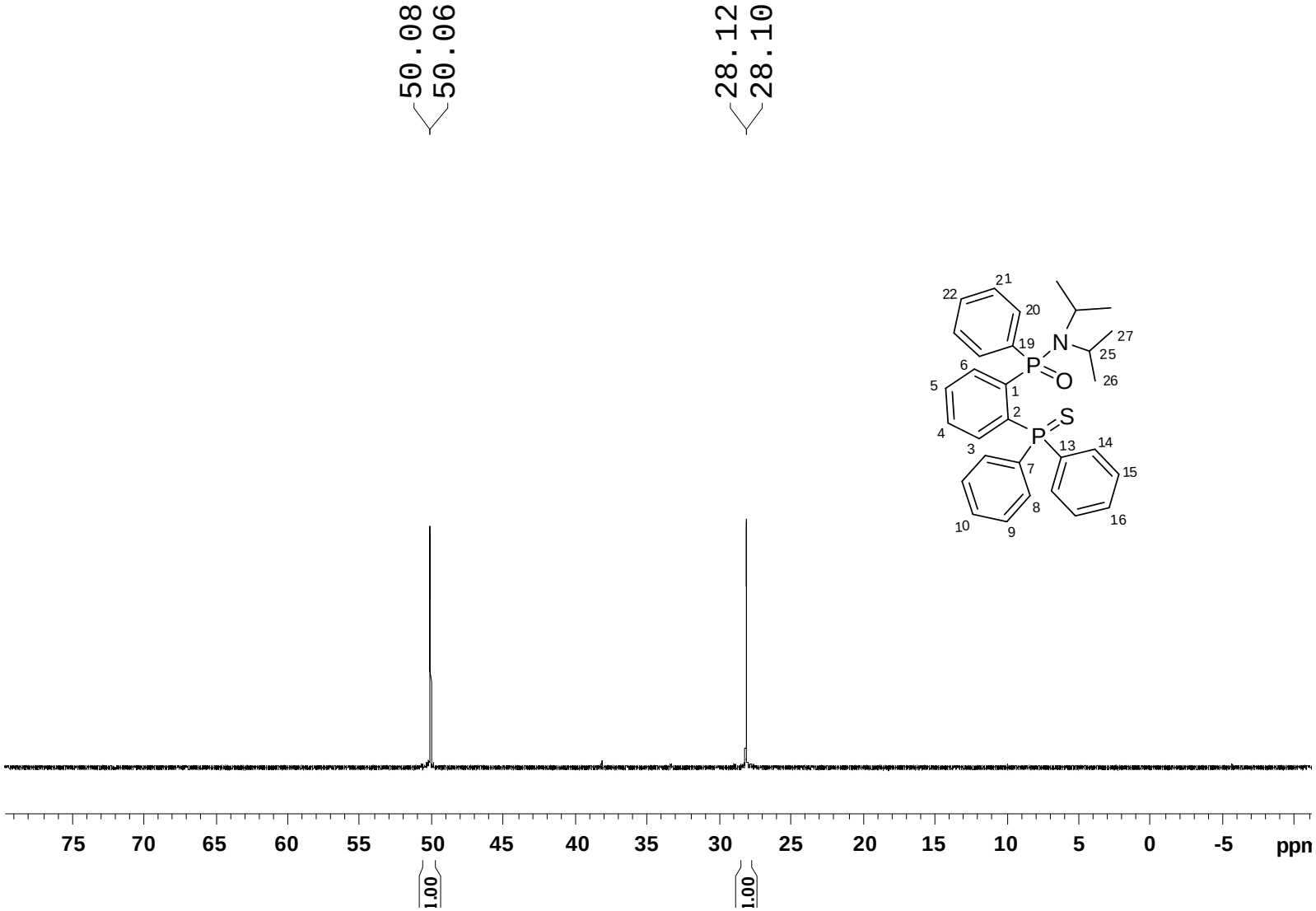

Figure S12. $^{31}P\{^{1}H\}$-NMR spectrum of ligand **20b.**

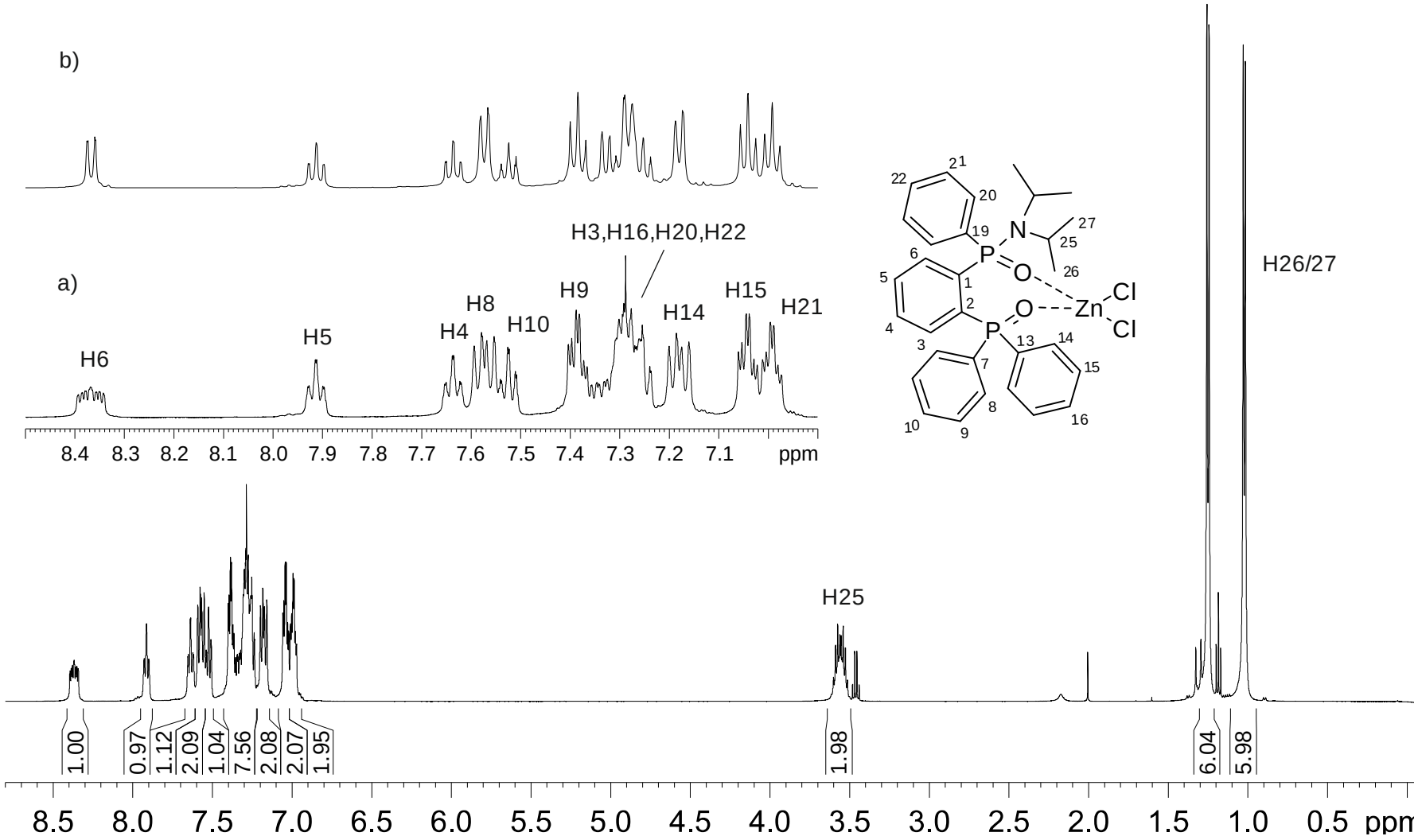

Figure S13. (a) ^{1}H- and (b) ^{1}H $\{^{31}$P$\}$-NMR spectra of complex **21a.**

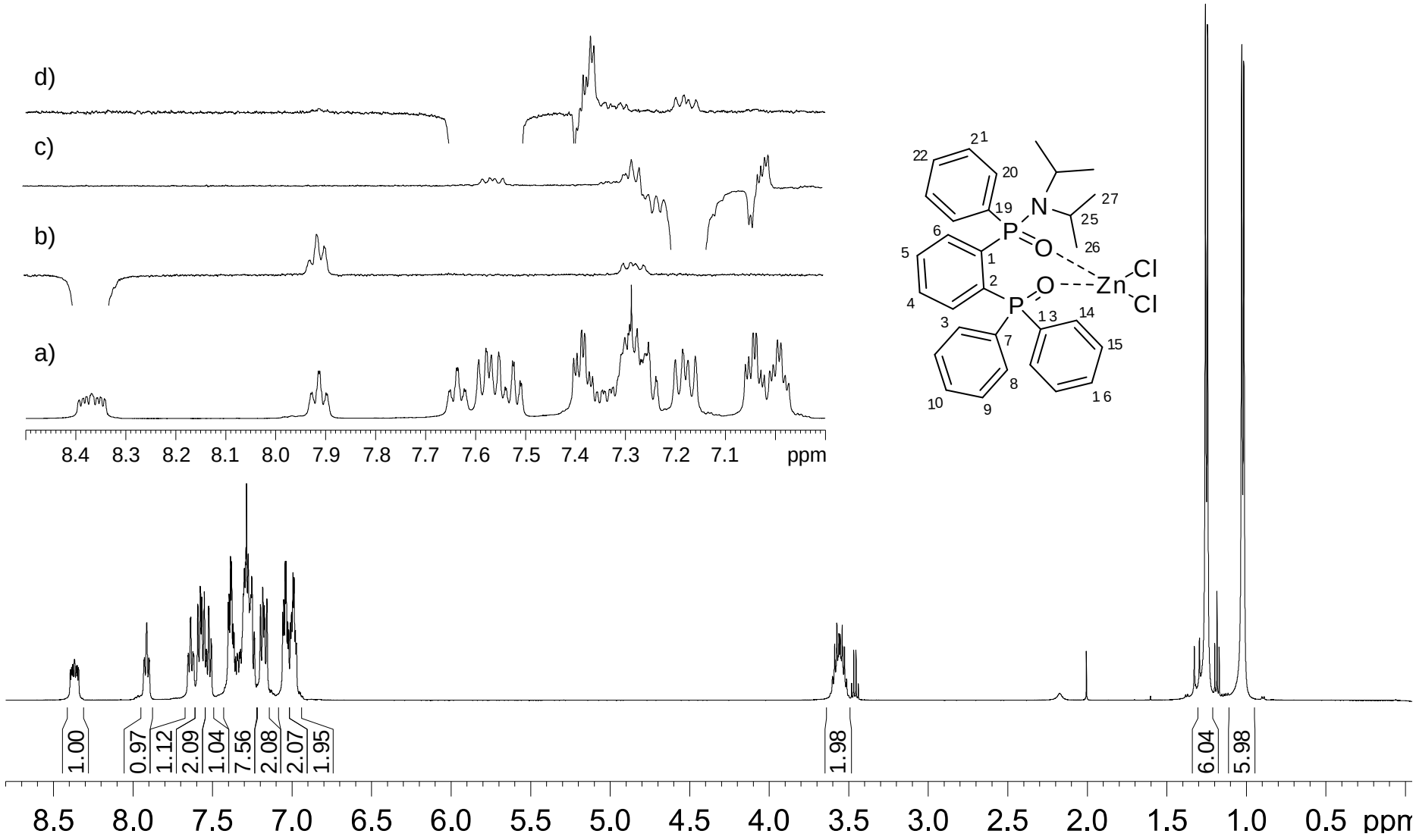

Figure S14. (a) ^{1}H-NMR and (b - d) 1D-NOESY (aromatic region) NMR spectra of complex **21a** with selective inversion of (b) H6 at δ 8.37 ppm, (c) H14 at δ 7.18 ppm and (d) H8 at δ 7.57 ppm).

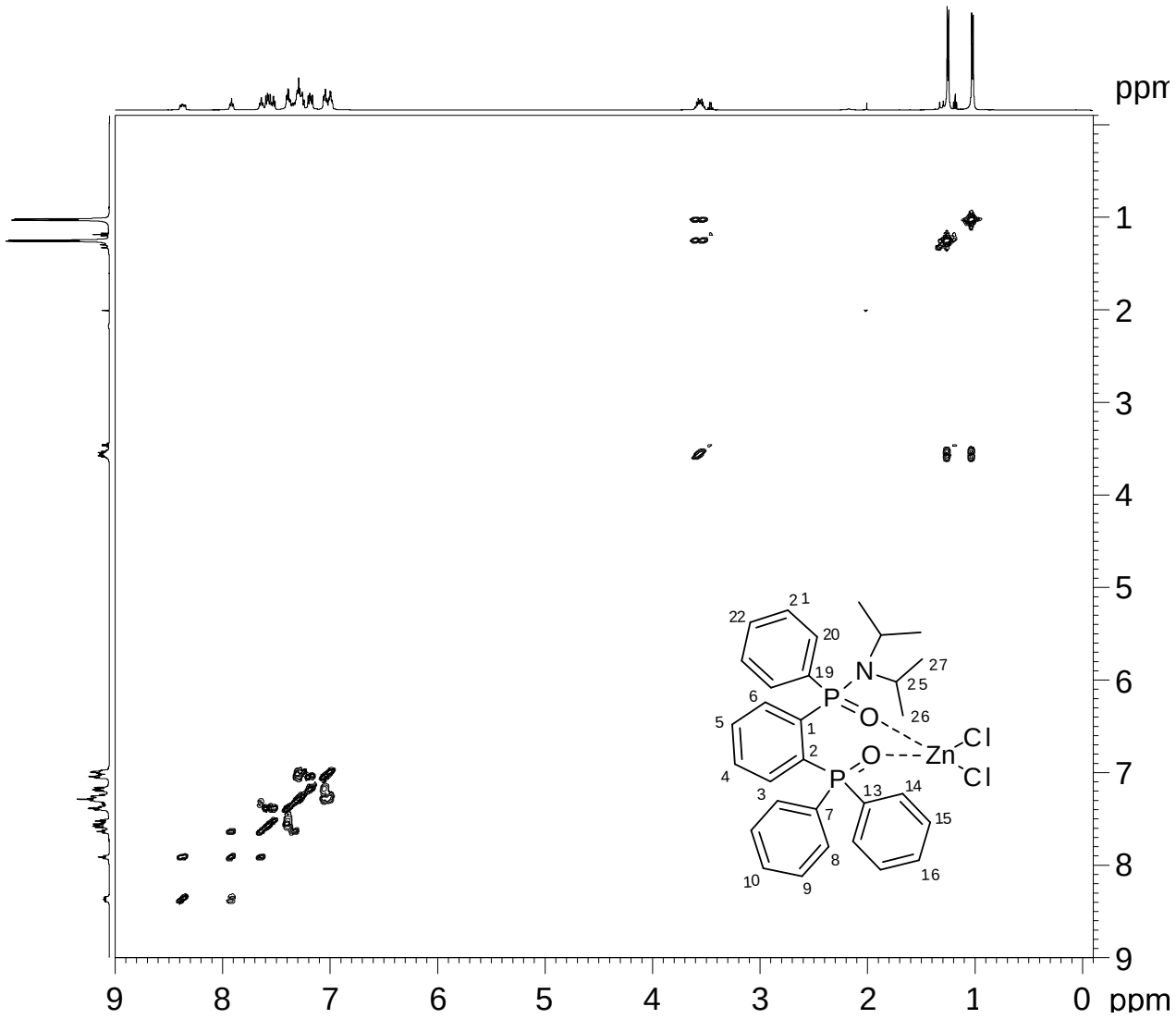

Figure S15. ^{1}H,^{1}H-COSY45 spectrum of complex **21a.**

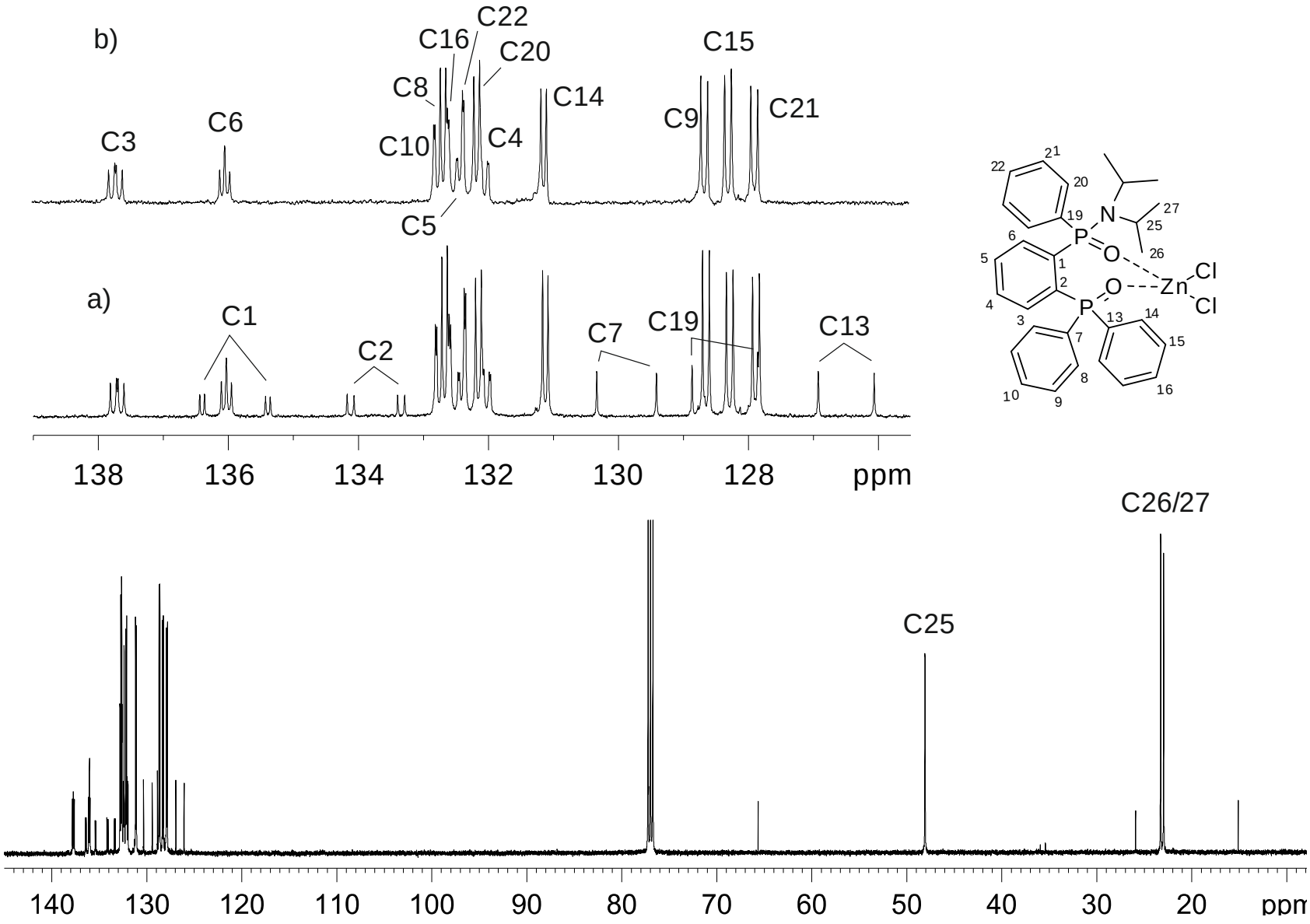

Figure S16. (a) $^{13}C\{^{1}H\}$- and (b) dept135 (aromatic region) NMR spectra of complex **21a.**

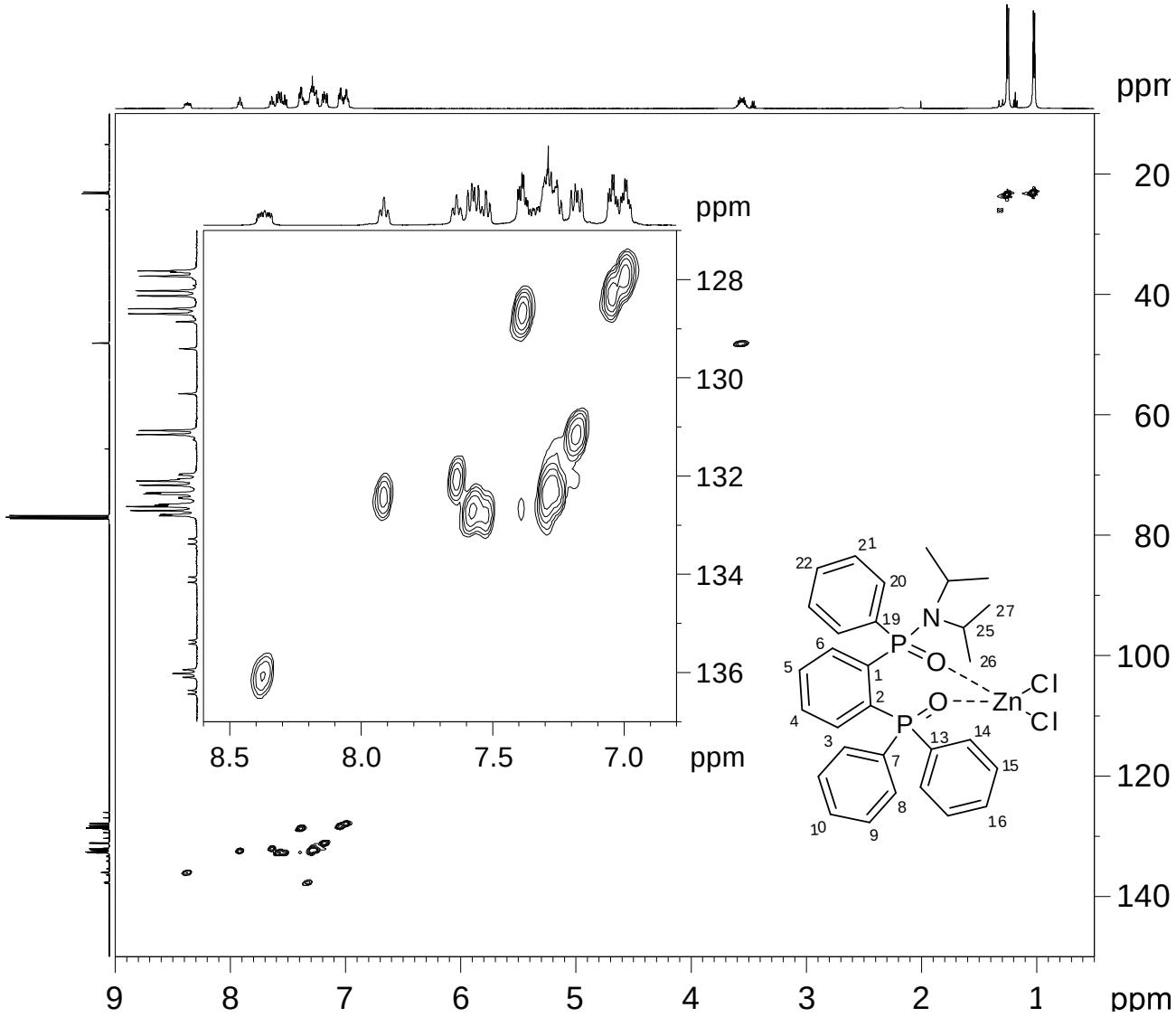

Figure S17. $^{1}H,^{13}C$-HSQC spectrum of complex **21a** including an expansion of the aromatic region.

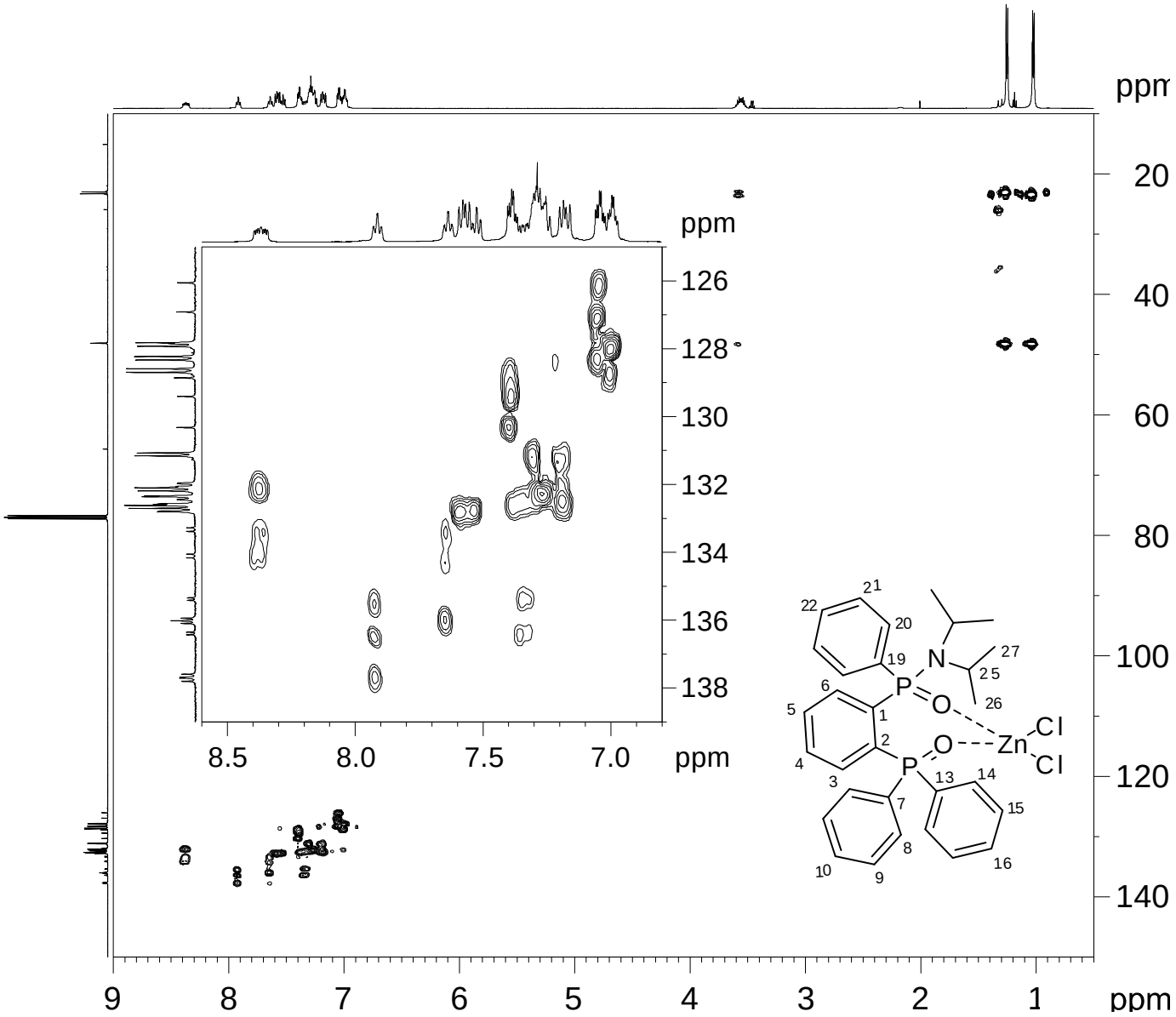

Figure S18. $^{1}H,^{13}C$-HMBC spectrum of complex **21a** including an expansion of the aromatic region**.**

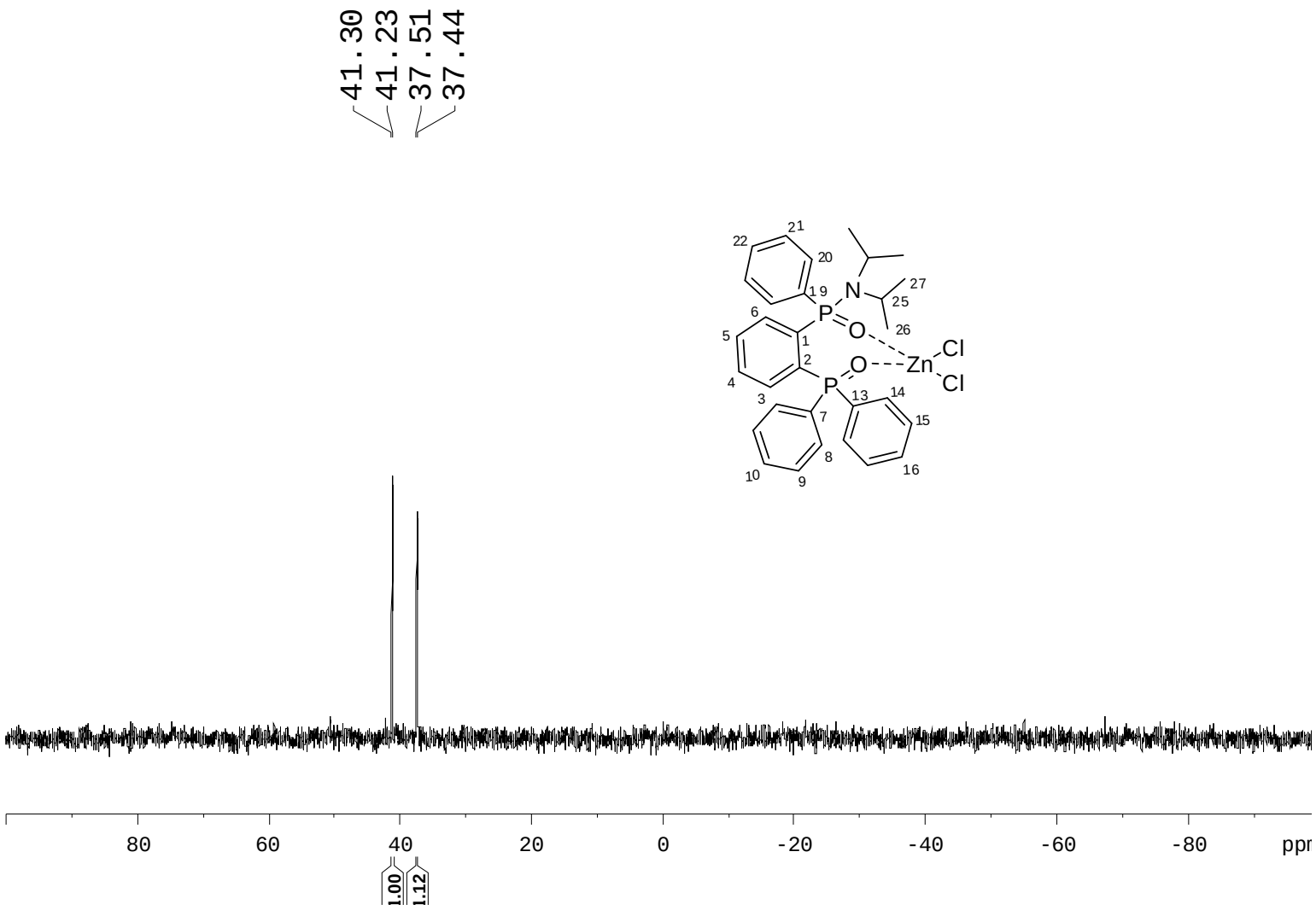

Figure S19. $^{31}P\{^{1}H\}$-NMR spectrum of complex **21a.**

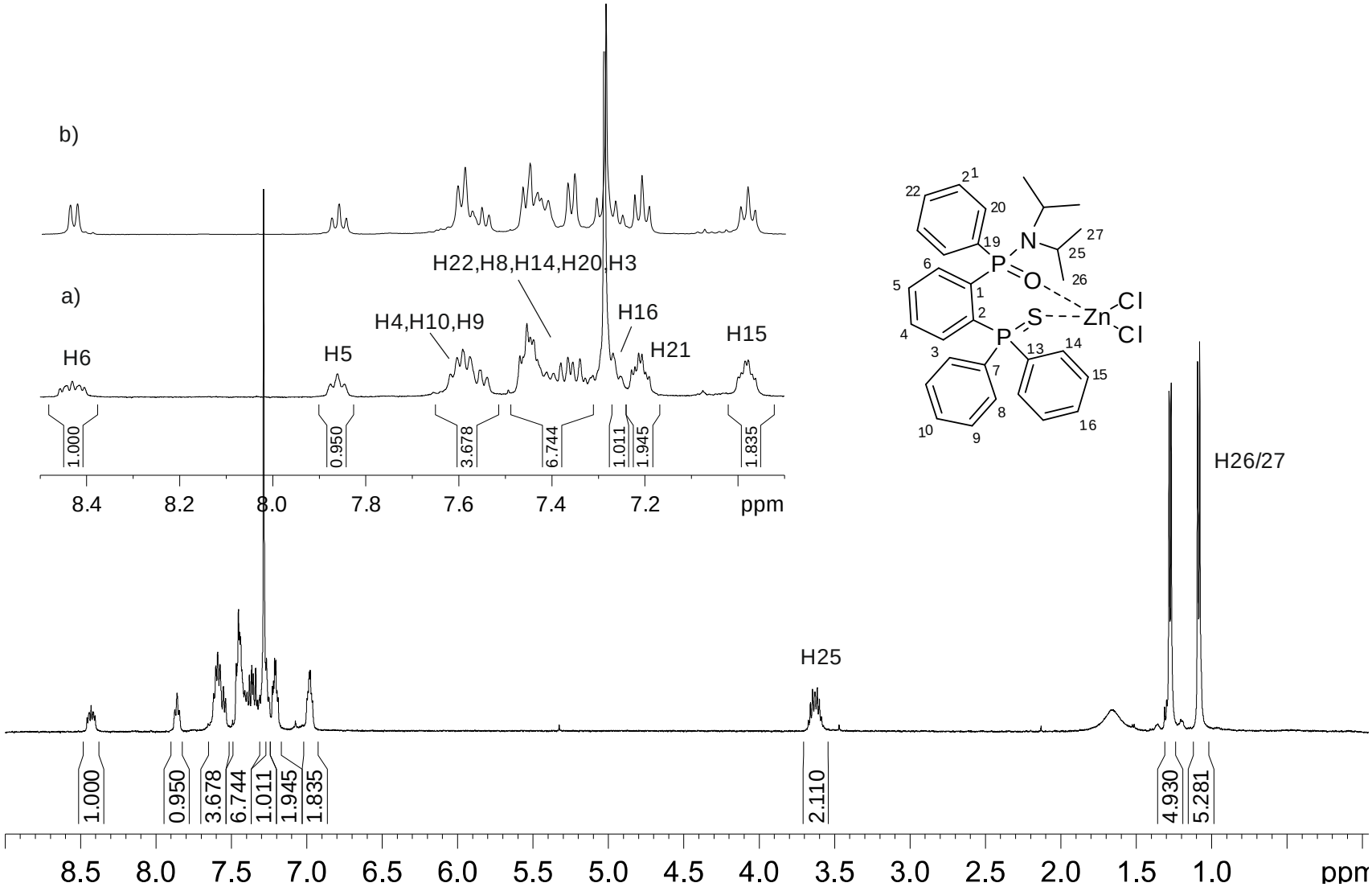

Figure S20. (a) ^{1}H- and (b) ^{1}H $\{^{31}$P$\}$-NMR spectra of complex **21b.**

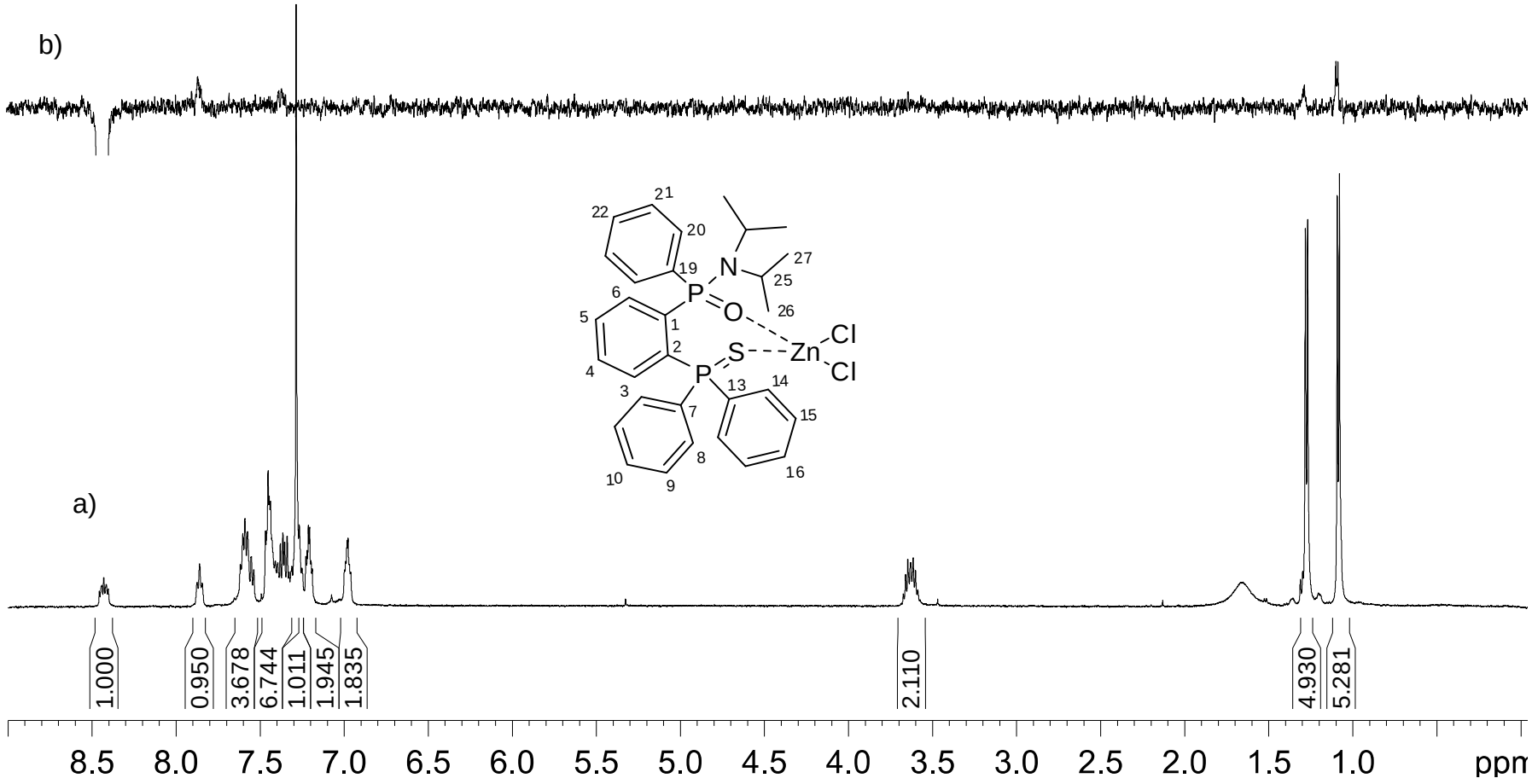

Figure S21. (a) ^{1}H-NMR and (b) 1D-NOESY (selective inversion of H6 at δ 8.43 ppm) NMR spectra of complex **21b.**

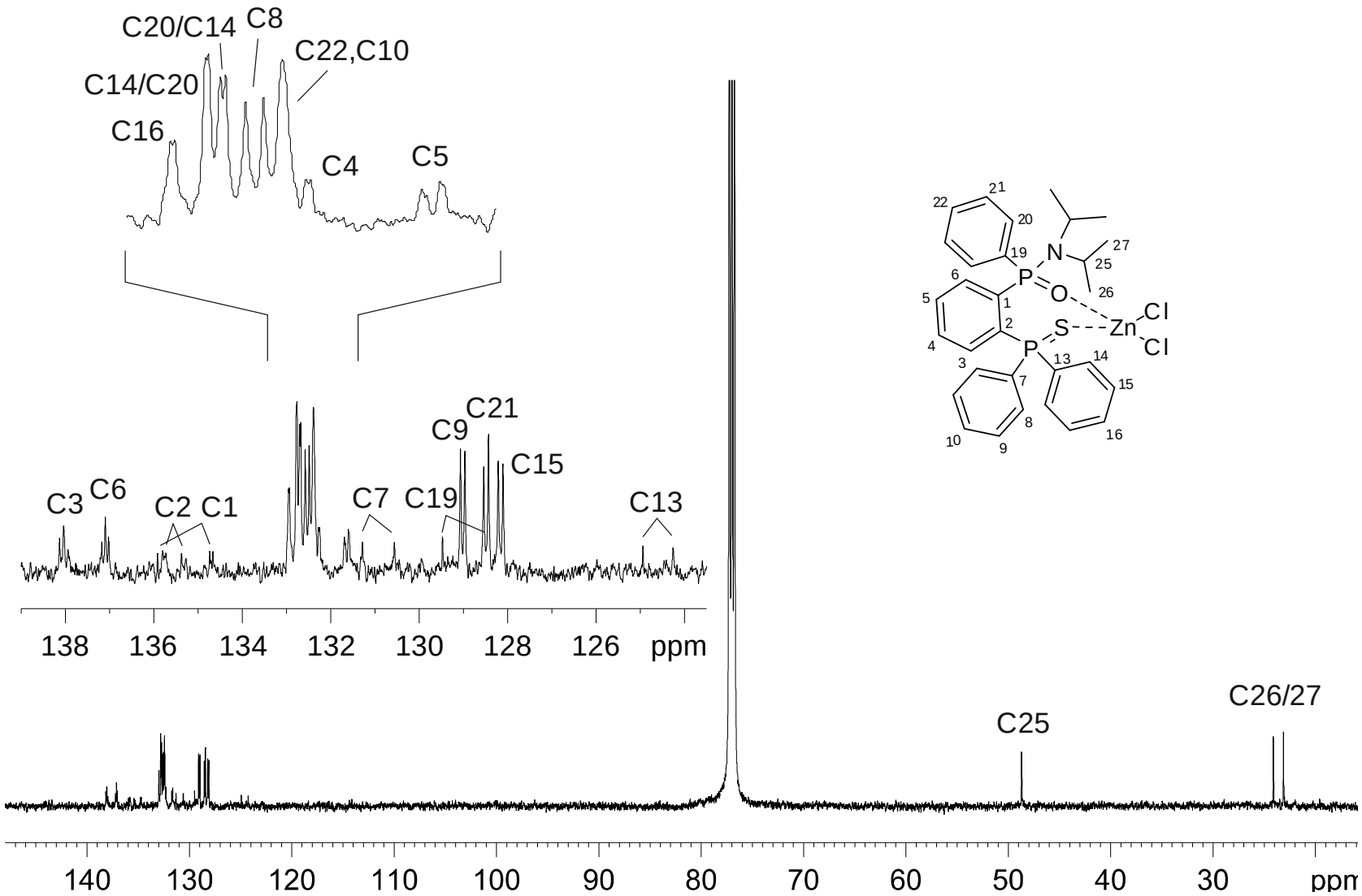

Figure S22. $^{13}C\{^{1}H\}$-NMR spectrum of complex **21b.**

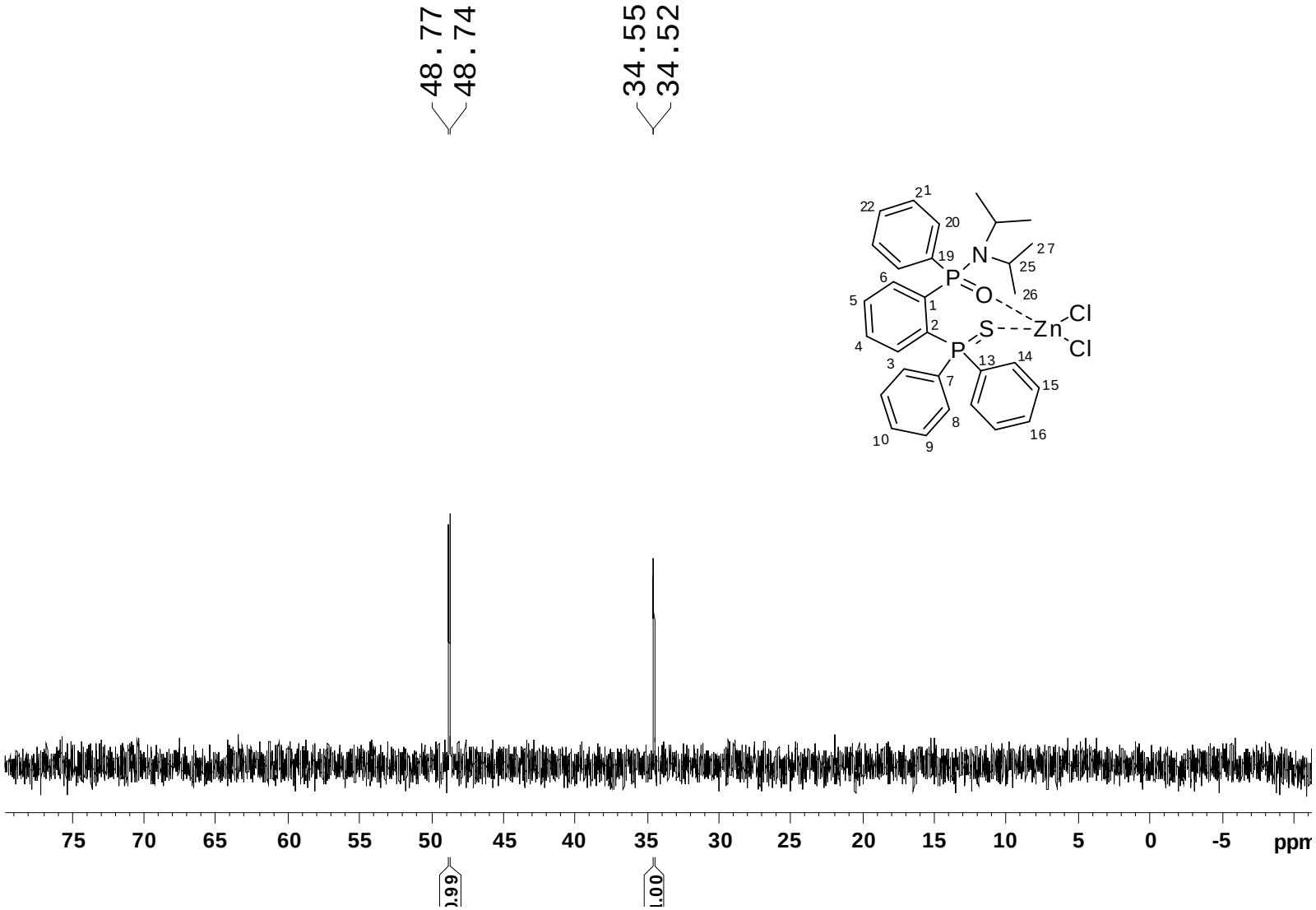

Figure S23. $^{31}P\{^{1}H\}$-NMR spectrum of complex **21b.**

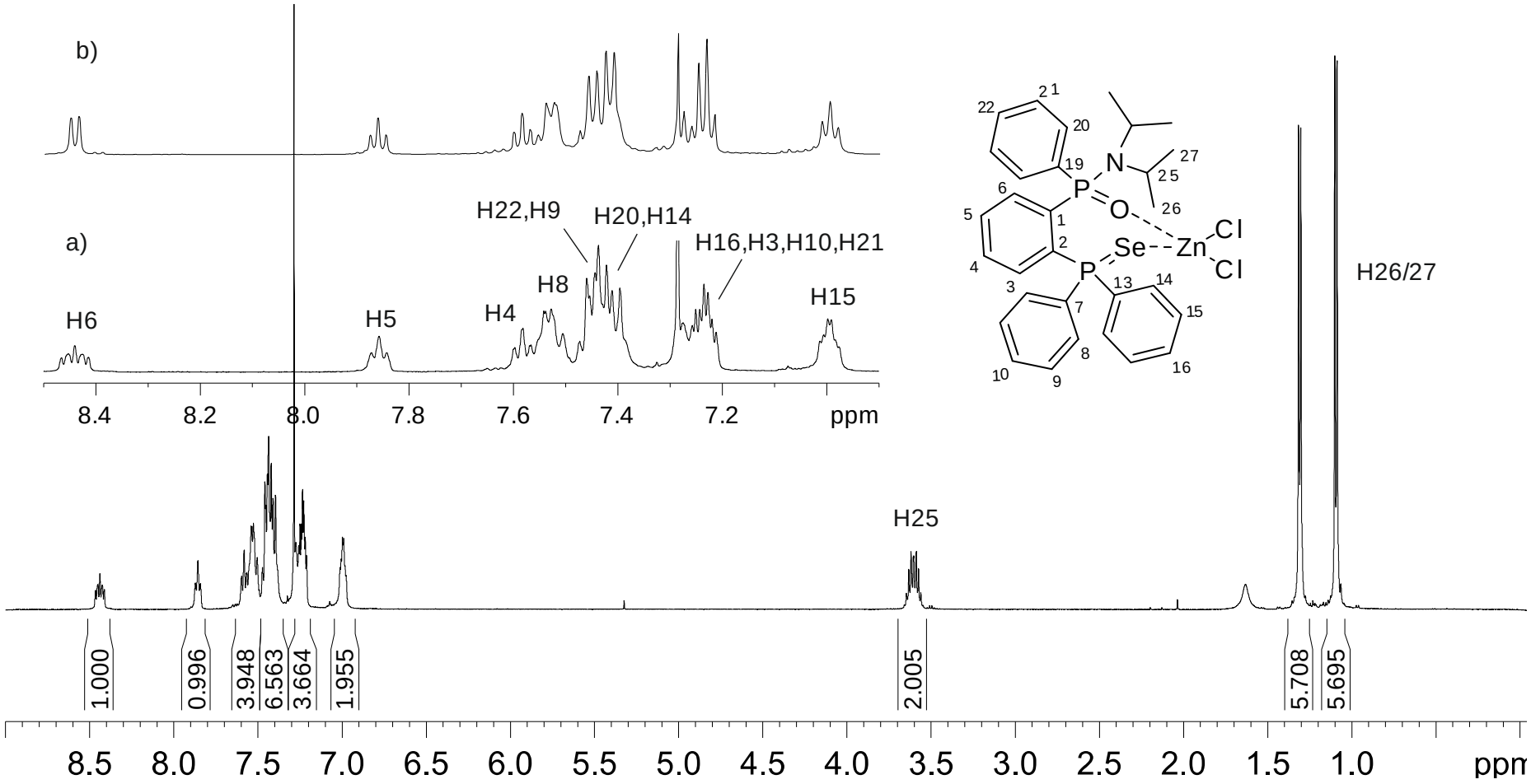

Figure S24. (a) ^{1}H- and (b) ^{1}H $\{^{31}$P$\}$-NMR spectra of complex **21c.**

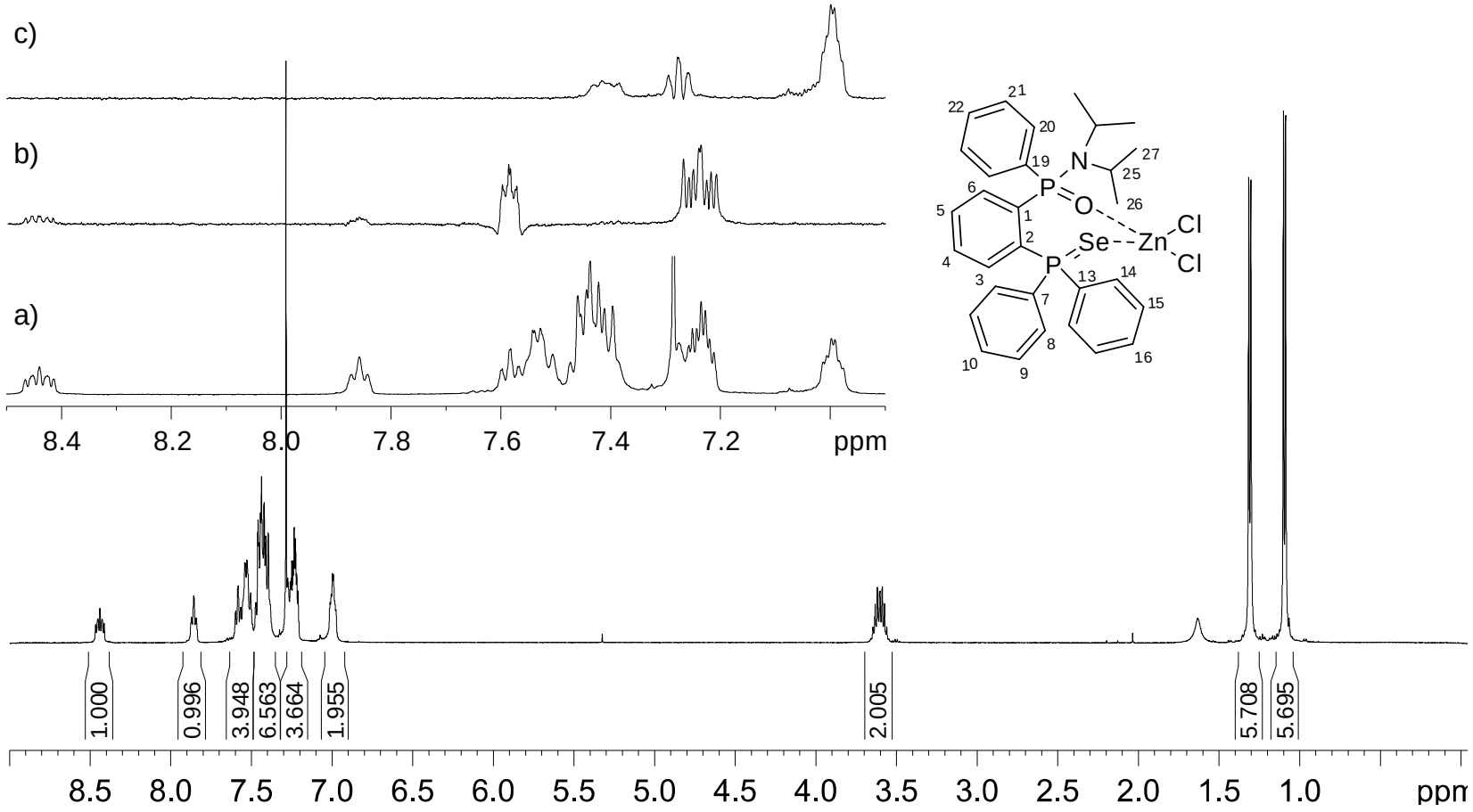

Figure S25. (a) ^{1}H-NMR and (b – c) 1D-TOCSY spectra of complex **21c** with selective excitation of (b) H6 at δ 8.44 ppm and (c) H15 at δ 6.99 ppm**.**

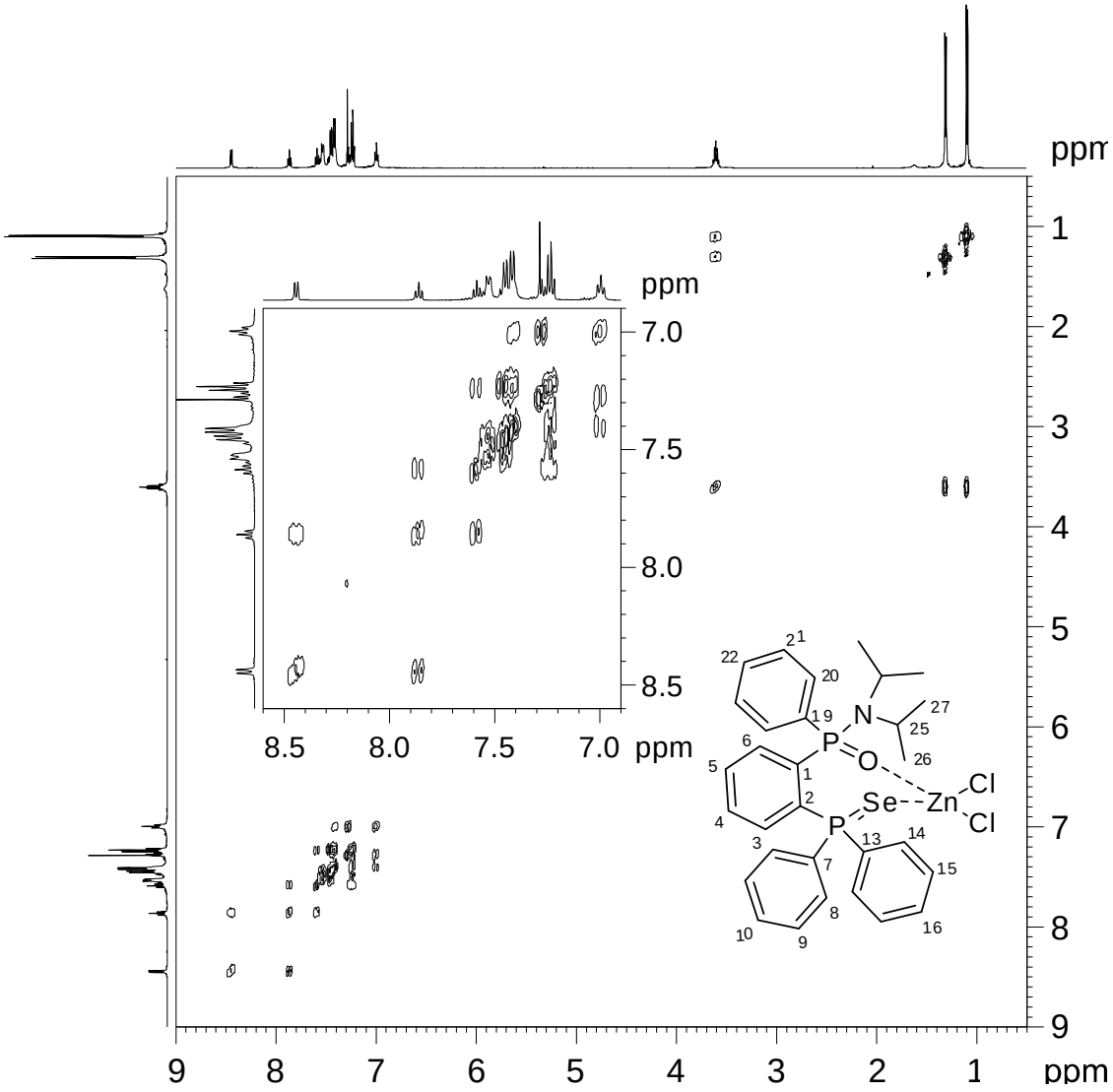

Figure S26. ^{1}H,^{1}H-COSY45 spectrum of complex **21c** including an expansion of the aromatic region**.**

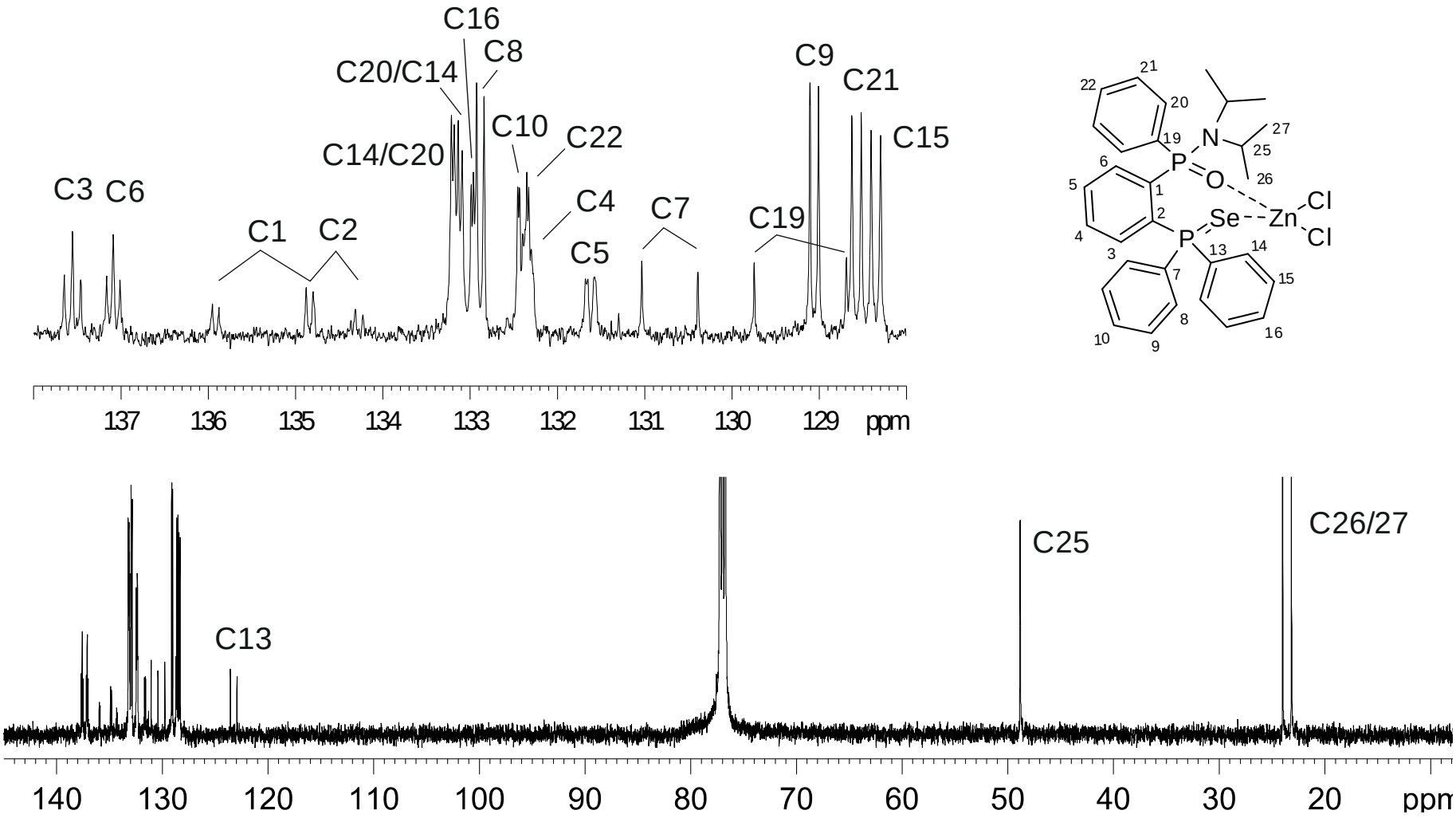

Figure S27. $^{13}C\{^{1}H\}$-NMR spectrum of complex **21c.**

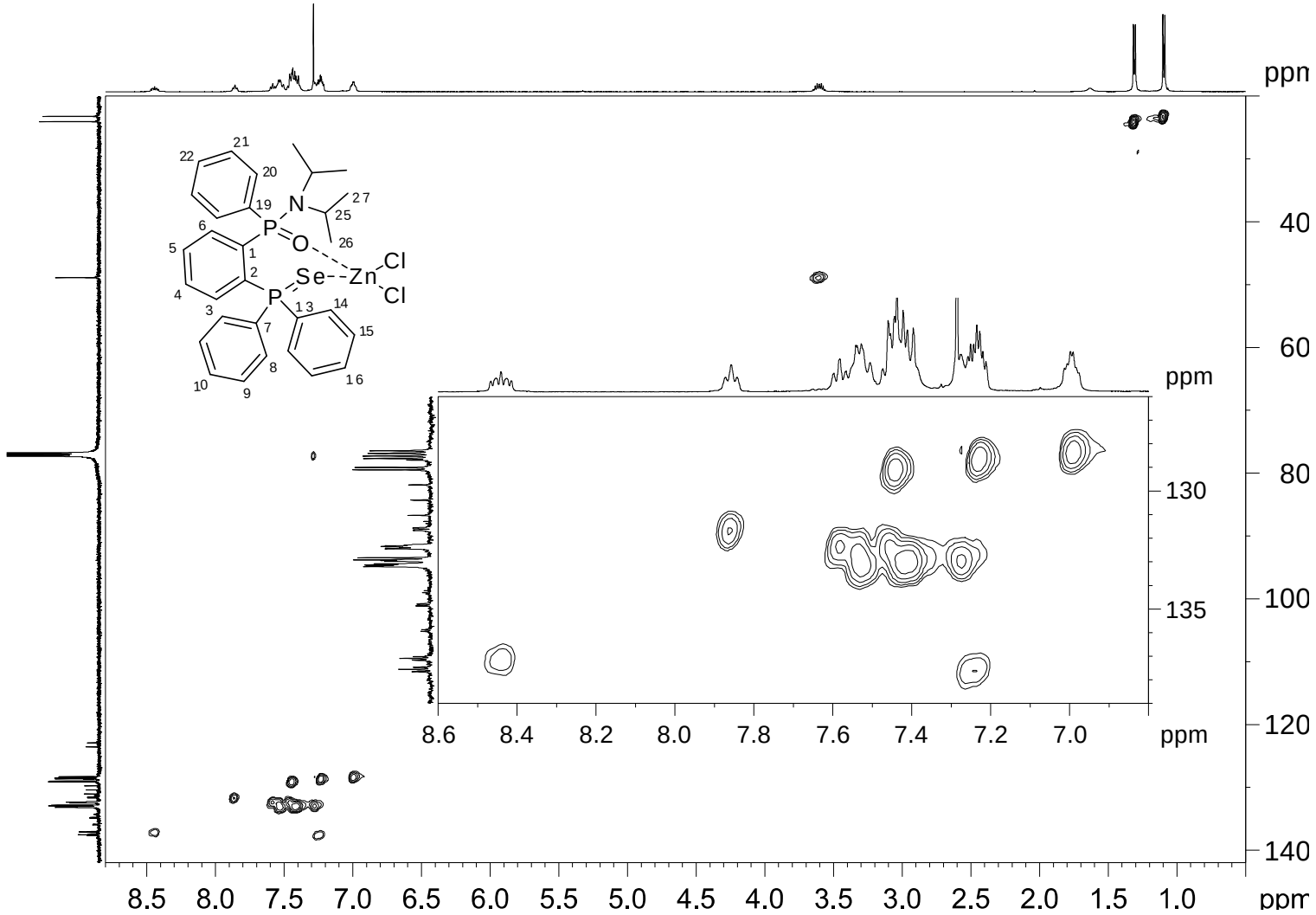

Figure S28. $^{1}H,^{13}C$-HSQC spectrum of complex **21c** including an expansion of the aromatic region**.**

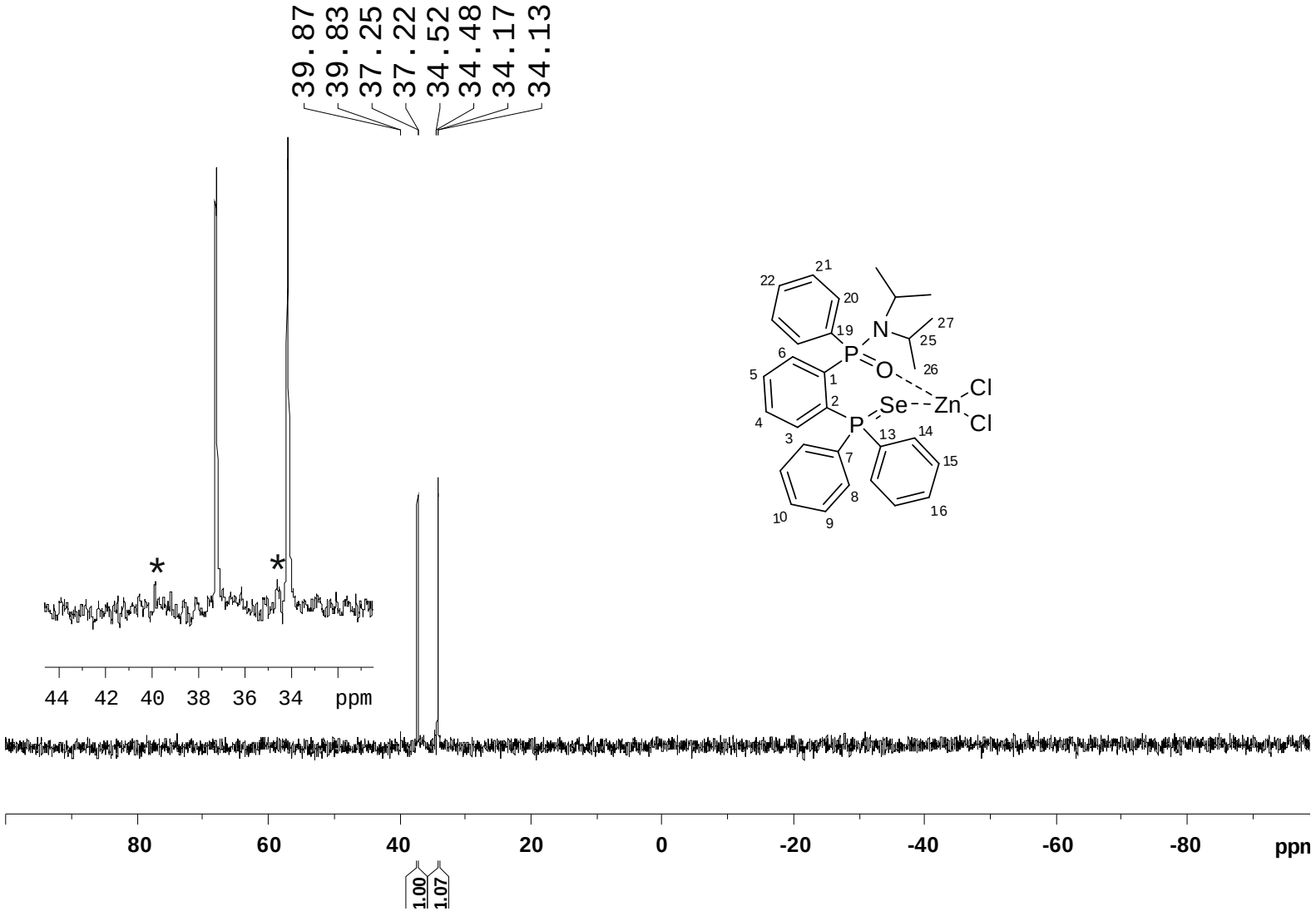

Figure S29. $^{31}P\{^{1}H\}$-NMR spectrum of complex **21c**. The ^{77}Se satellites are indicated by an asterisc.

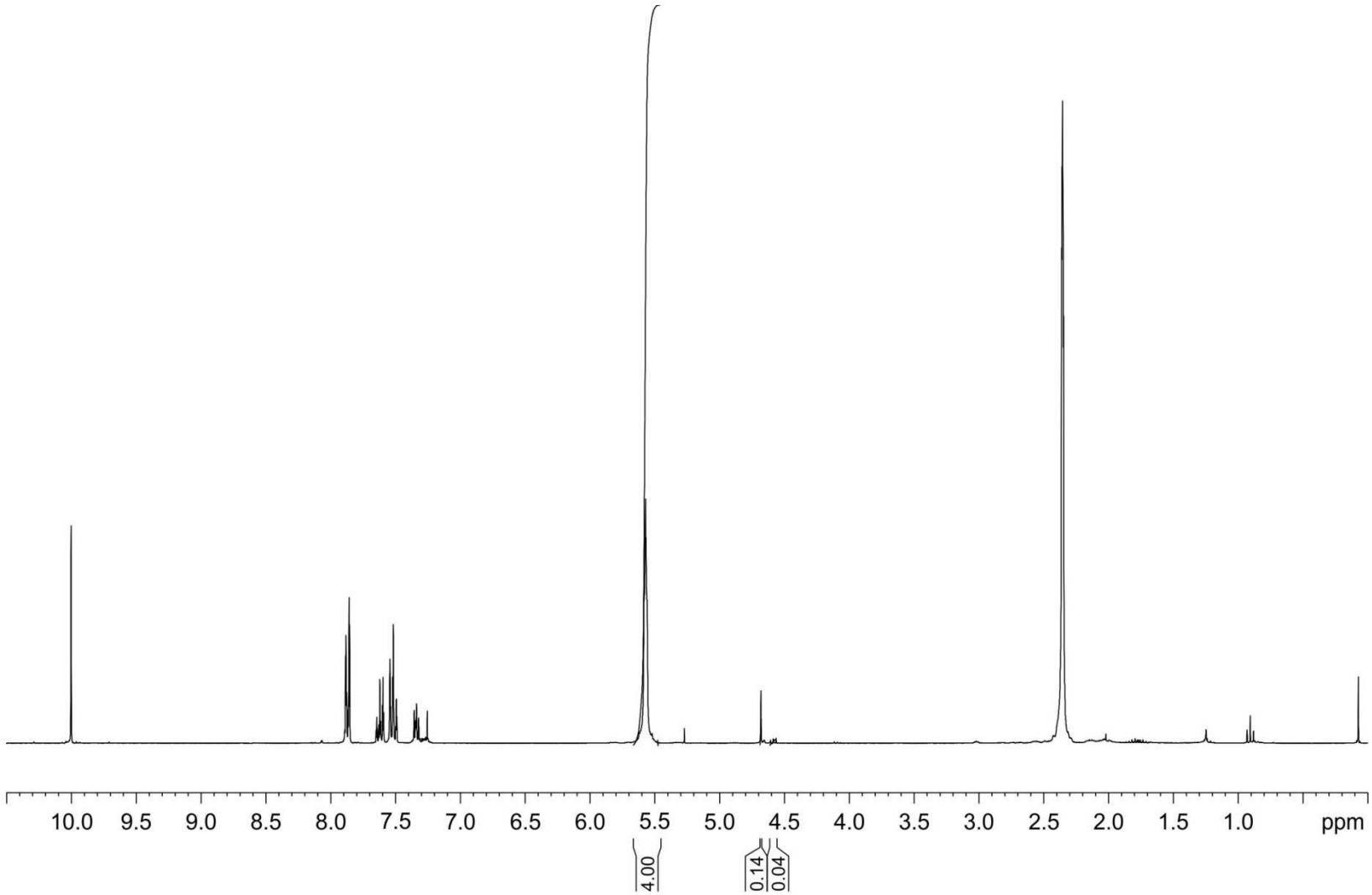

Figure S30. ^{1}H-NMR spectrum of the crude reaction mixture of the addition of Et_2Zn to benzaldehyde in the absence of ligand. Reaction time of 1.5 h. The integrals shown correspond to the internal standard (COD), the benzylic alcohol (14%) and adduct **22a** (4%).

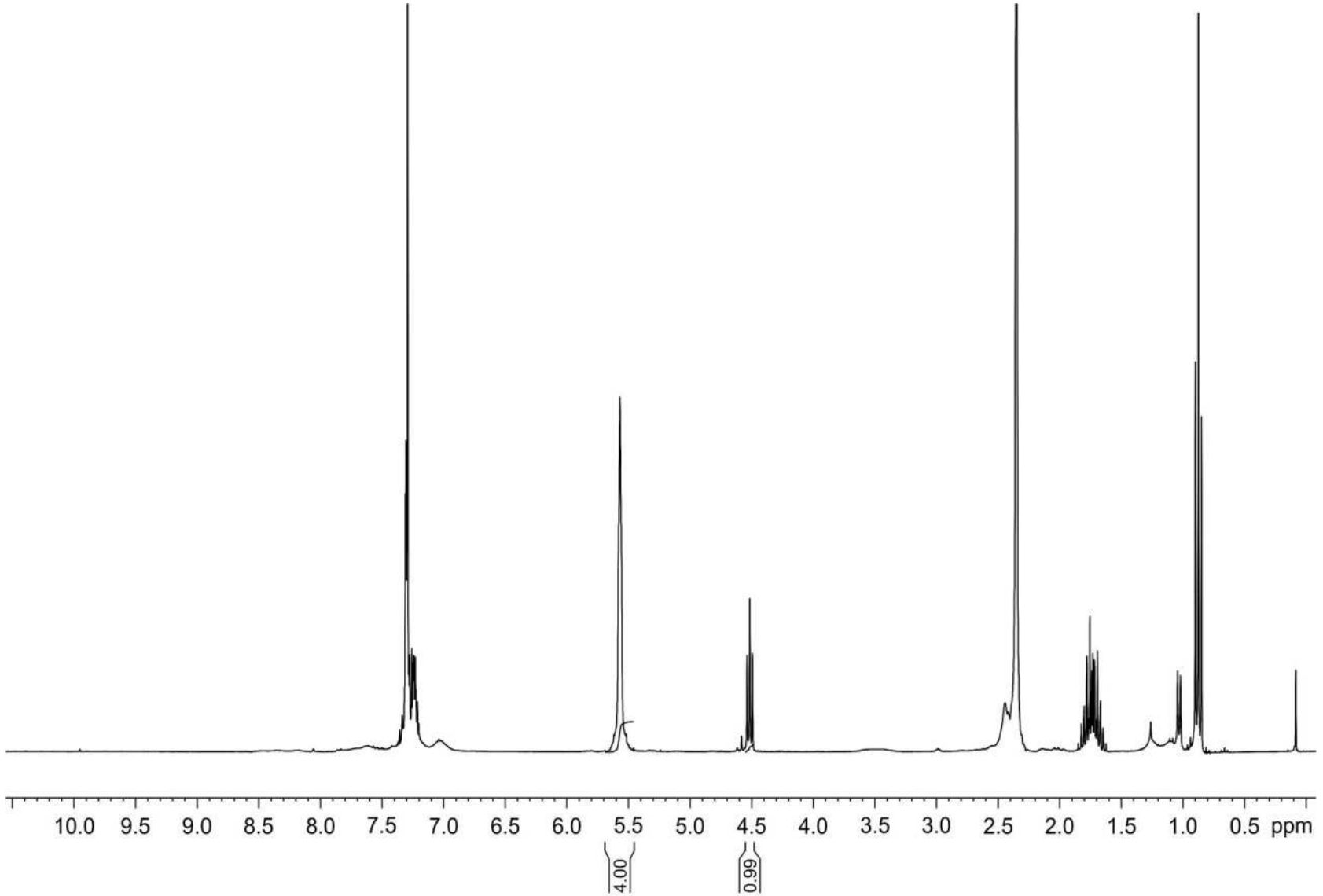

Figure S31. ^{1}H-NMR spectrum of the crude reaction mixture of the addition of Et_2Zn to benzaldehyde in the presence of ligand **20a** (10 mol%). Reaction time of 1.5 h. The integrals shown correspond to the internal standard (COD) and the adduct **22a** (99%).

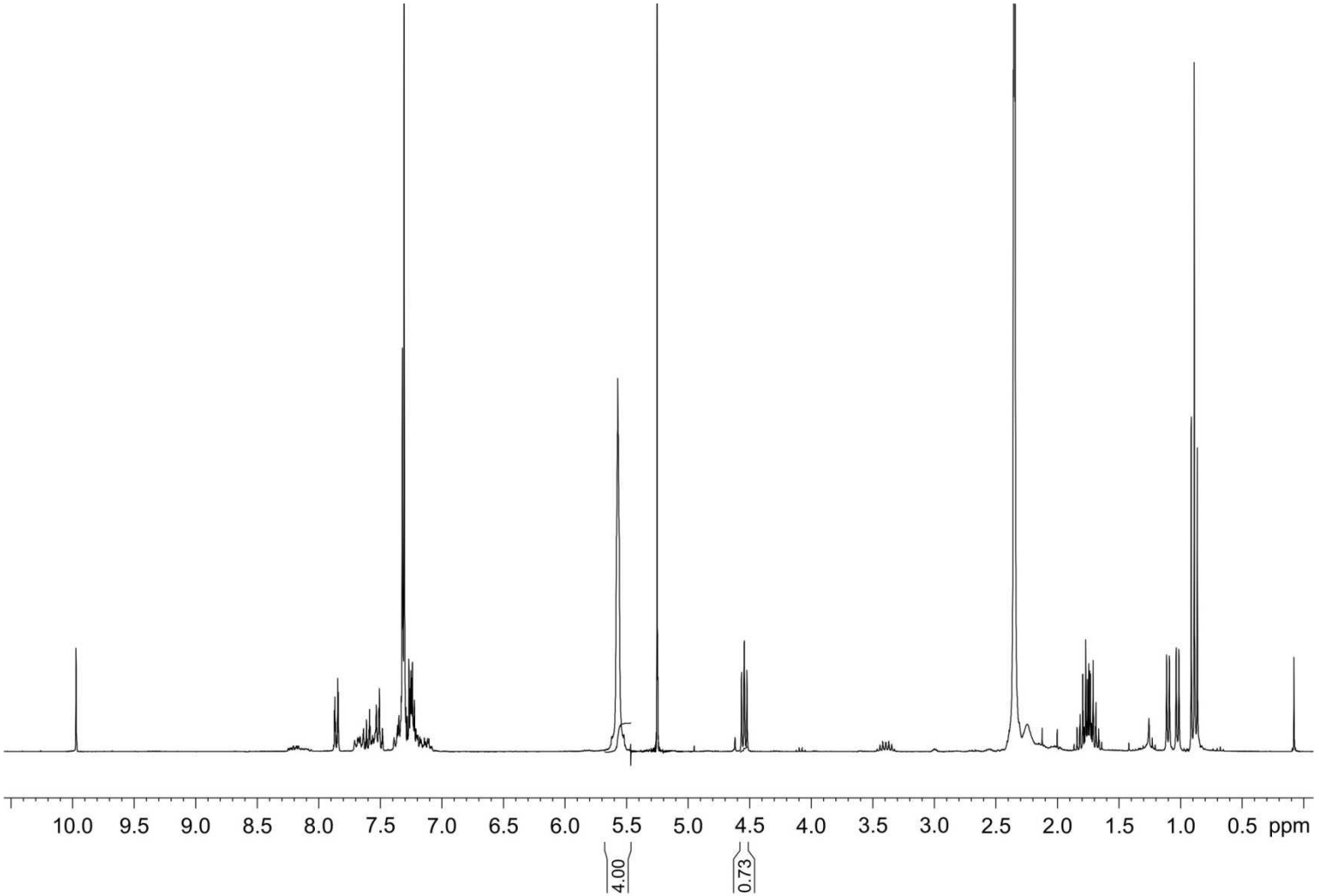

Figure S32. ^{1}H-NMR spectrum of the crude reaction mixture of the addition of Et_2Zn to benzaldehyde in the presence of ligand **20b** (10 mol%). Reaction time of 1.5 h. The integrals shown correspond to the internal standard (COD) and the adduct **22a** (73%).

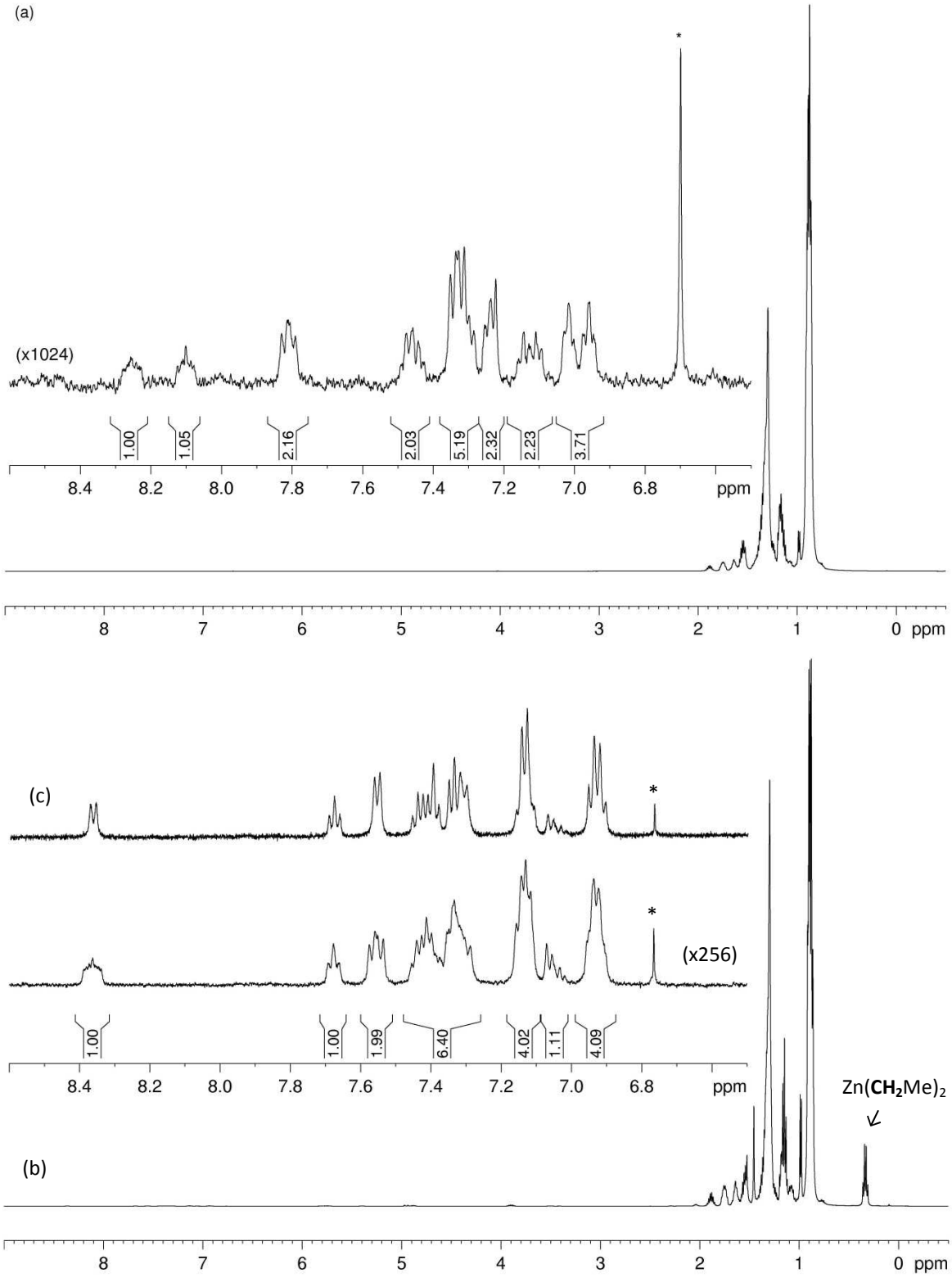

Figure S33. ^{1}H-NMR spectra of: (a) a saturated solution of **20a** in hexanes (NS 200, vertical scaling factor of 1024); (b) a saturated solution of complex **20a-ZnEt$_2$** (5.1 mg/mL) in a 1.0 M solution of Et_2Zn in hexanes (NS = 80, vertical scaling factor of 128); (c) expansion of the ^{1}H{^{31}P}-NMR spectrum of sample (b). Exponential multiplication by a LB =1 and base line correction were applied to all spectra. The asteriscs indicate the residual signal of $CDCl_3$ shielded by 0.54 ppm due to magnetic susceptibility differences.

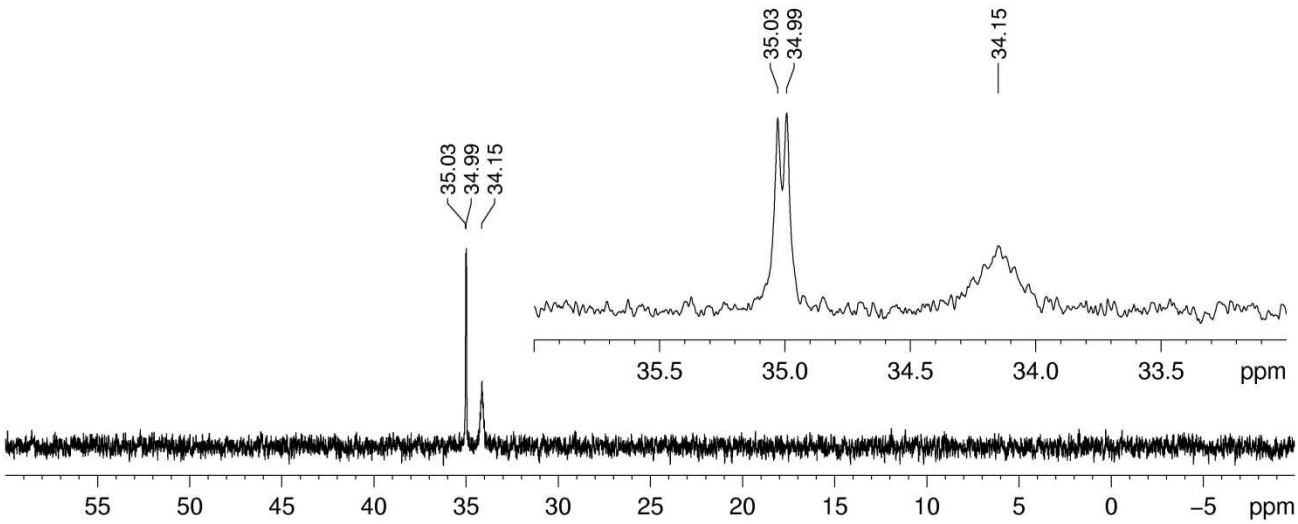

Figure S34. $^{31}P\{^{1}H\}$-NMR spectrum of a saturated solution of complex **20a-ZnEt$_2$** in a 1.0 M solution of Et_2Zn in hexanes (NS = 200, exponential multiplication of LB = 2).

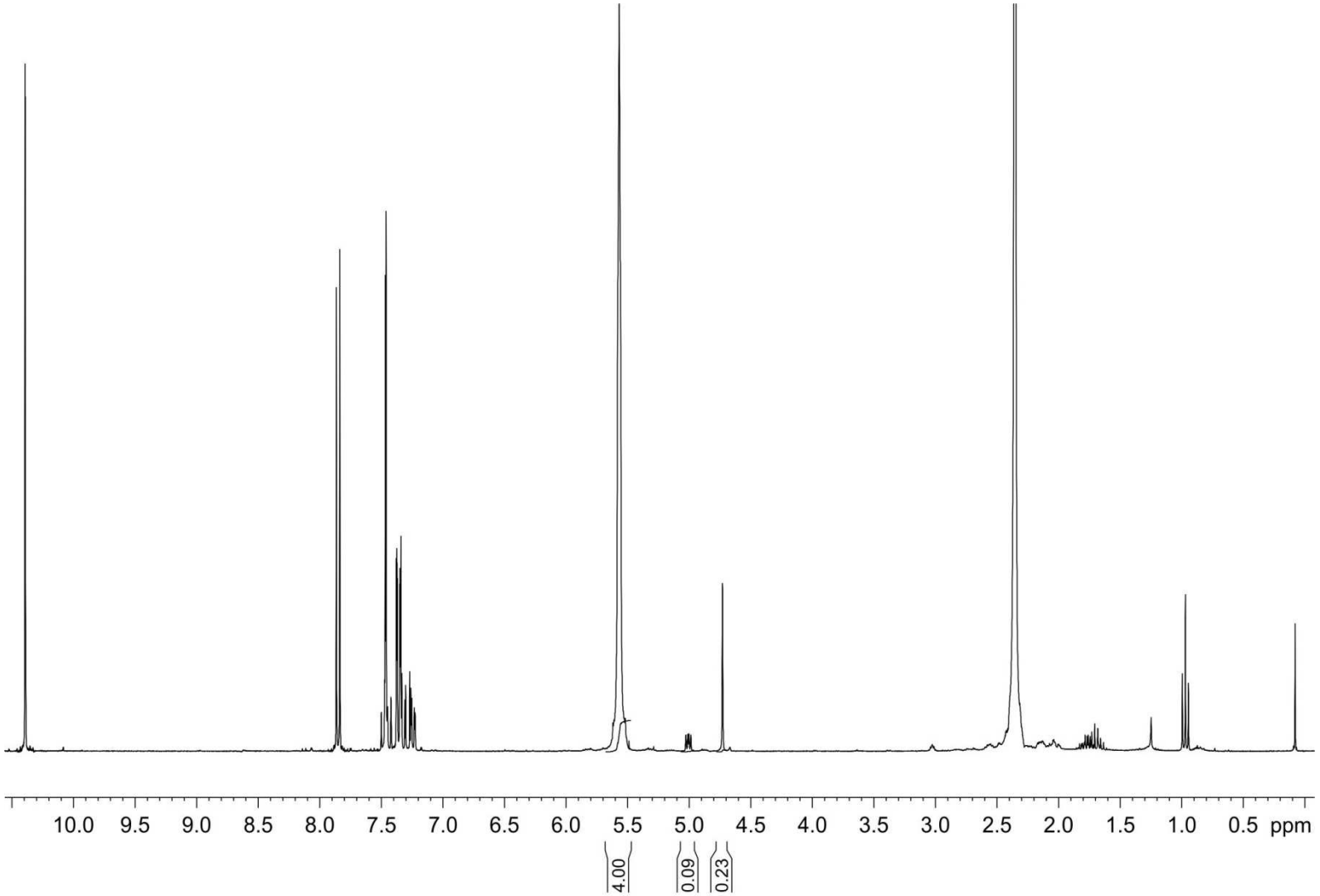

Figure S35. ^{1}H-NMR spectrum of the crude reaction mixture of the addition of Et_2Zn to 2,4-dichlorobenzaldehyde in the absence of ligand. Reaction time of 1 h. The integrals shown correspond to the internal standard (COD), (2,4-dichlorophenyl)methanol (23%) and adduct **22b** (9%).

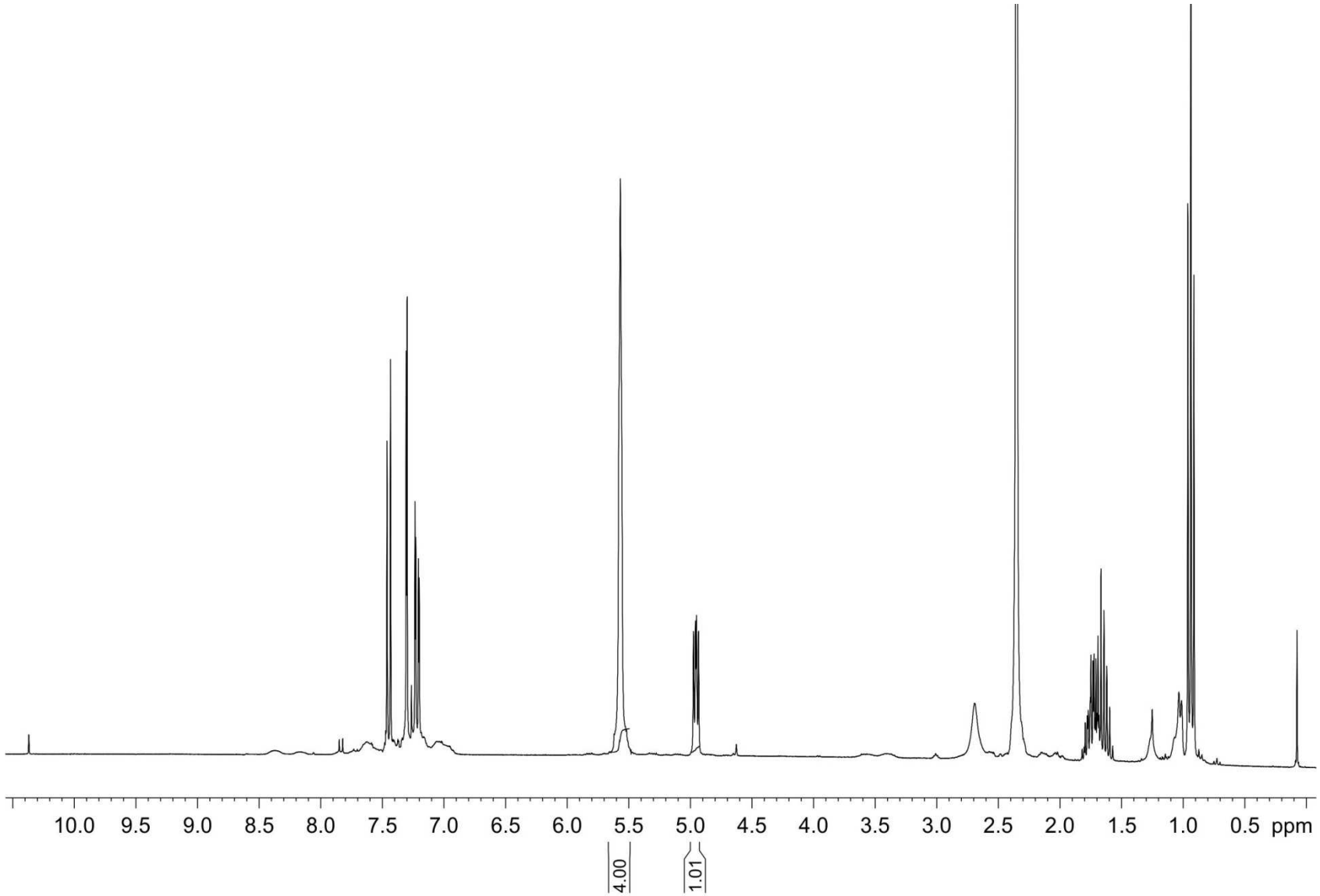

Figure S36. ^{1}H-NMR spectrum of the crude reaction mixture of the addition of Et_2Zn to 2,4-dichlorobenzaldehyde in the presence of ligand **20a** (10 mol%). Reaction time of 1 h. The integrals shown correspond to the internal standard (COD) and the adduct **22b** (100%).

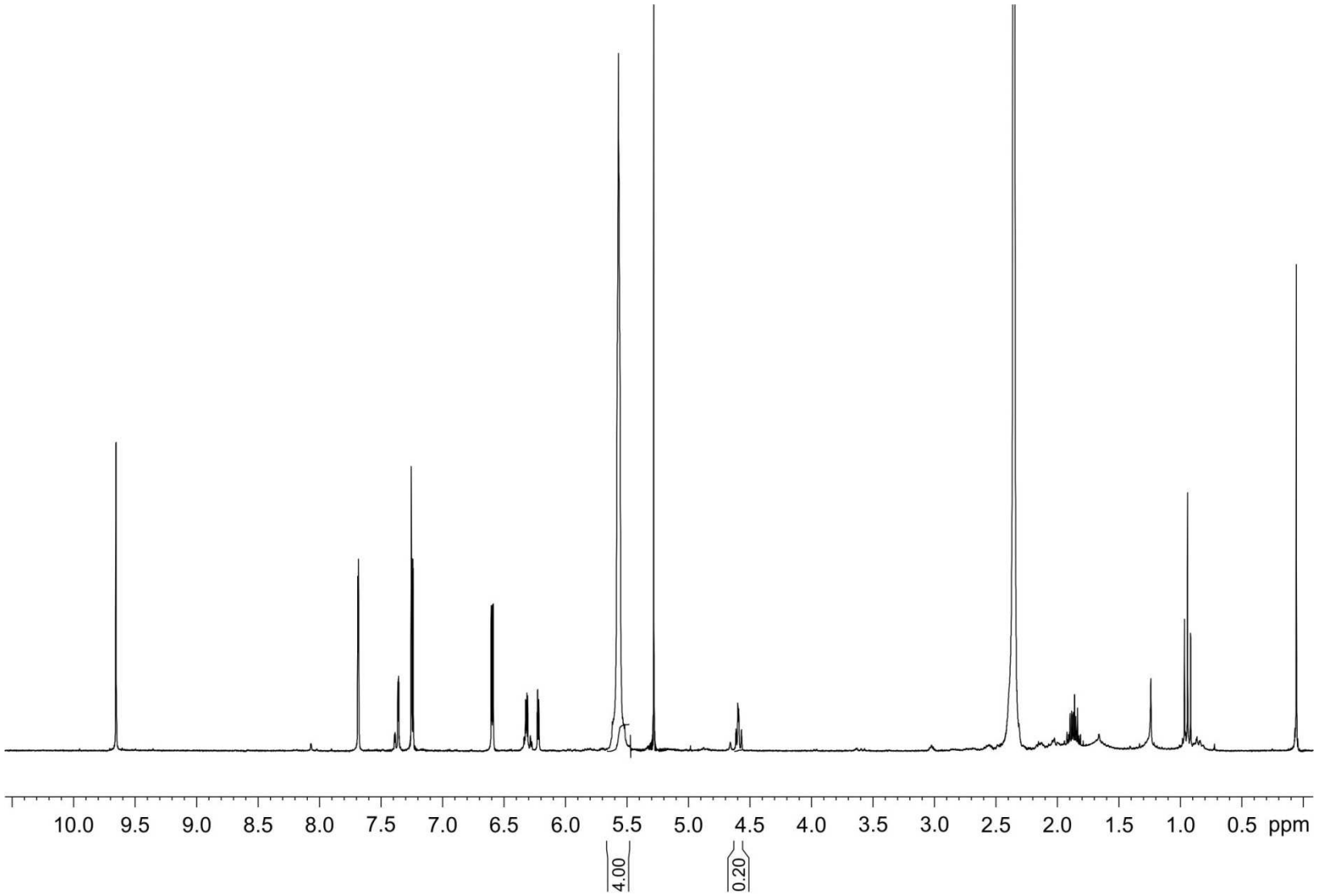

Figure S37. ^{1}H-NMR spectrum of the crude reaction mixture of the addition of Et_2Zn to 2-furaldehyde in the absence of ligand. Reaction time of 1 h. The integrals shown correspond to the internal standard (COD) and adduct **22c** (20%).

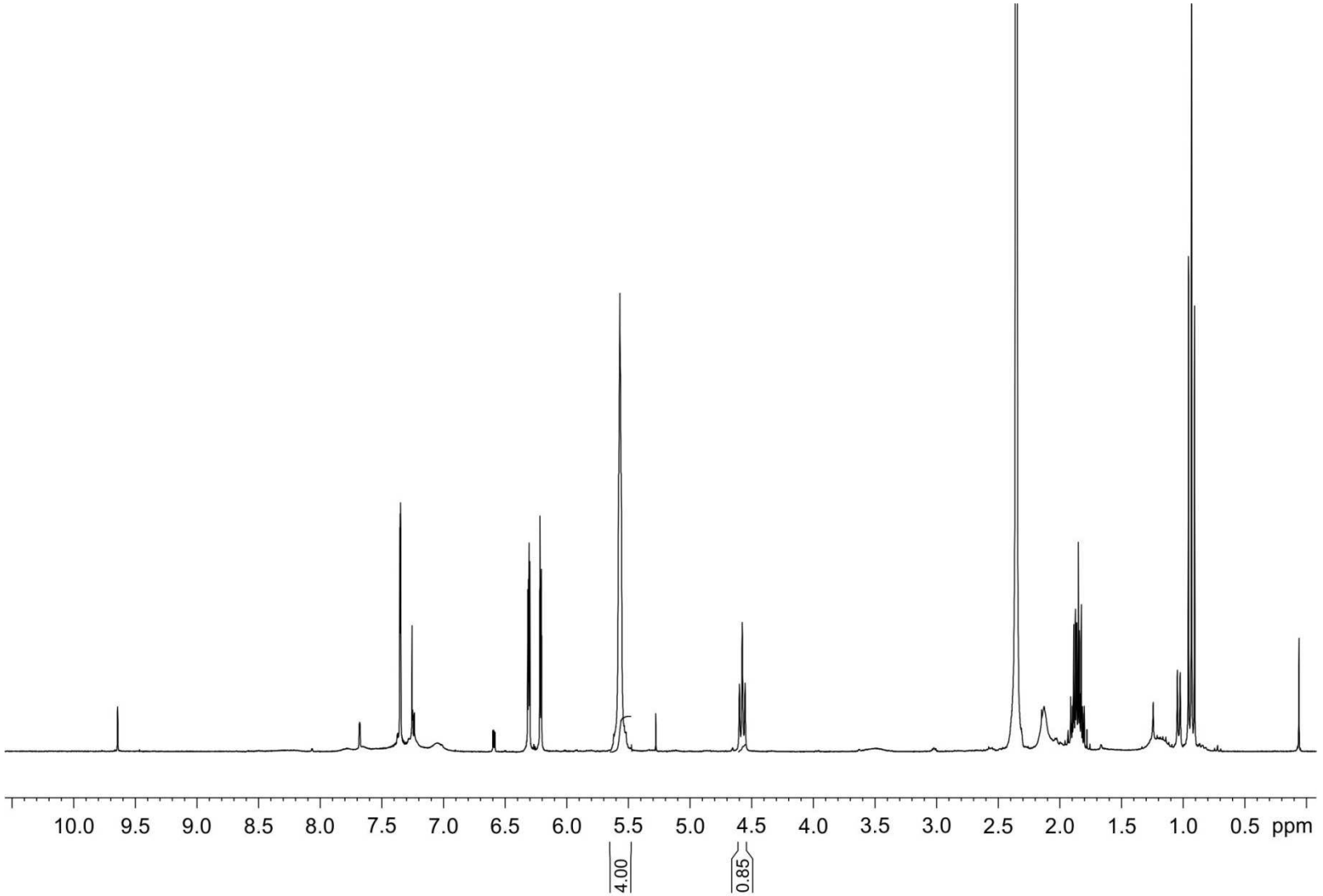

Figure S38. ^{1}H-NMR spectrum of the crude reaction mixture of the addition of Et_2Zn to 2-furaldehyde in the presence of ligand **20a** (10 mol%). Reaction time of 1h. The integrals shown correspond to the internal standard (COD) and the adduct **22c** (85%).

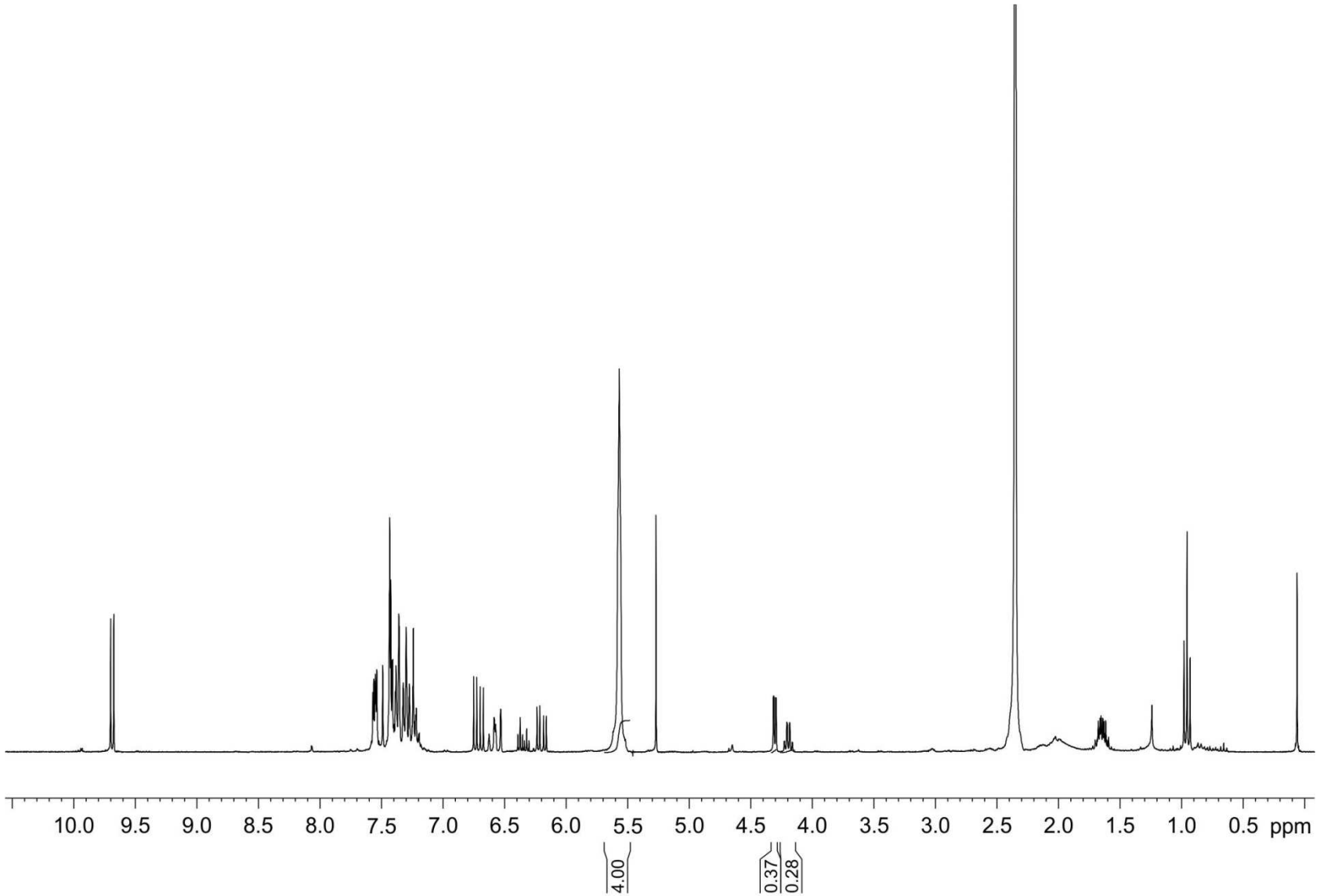

Figure S39. ^{1}H-NMR spectrum of the crude reaction mixture of the addition of Et_2Zn to cinnamaldehyde in the absence of ligand. Reaction time of 1.5 h. The integrals shown correspond to the internal standard (COD), (*E*)-3-phenylprop-2-en-1-ol (37%) and adduct **22d** (28%).

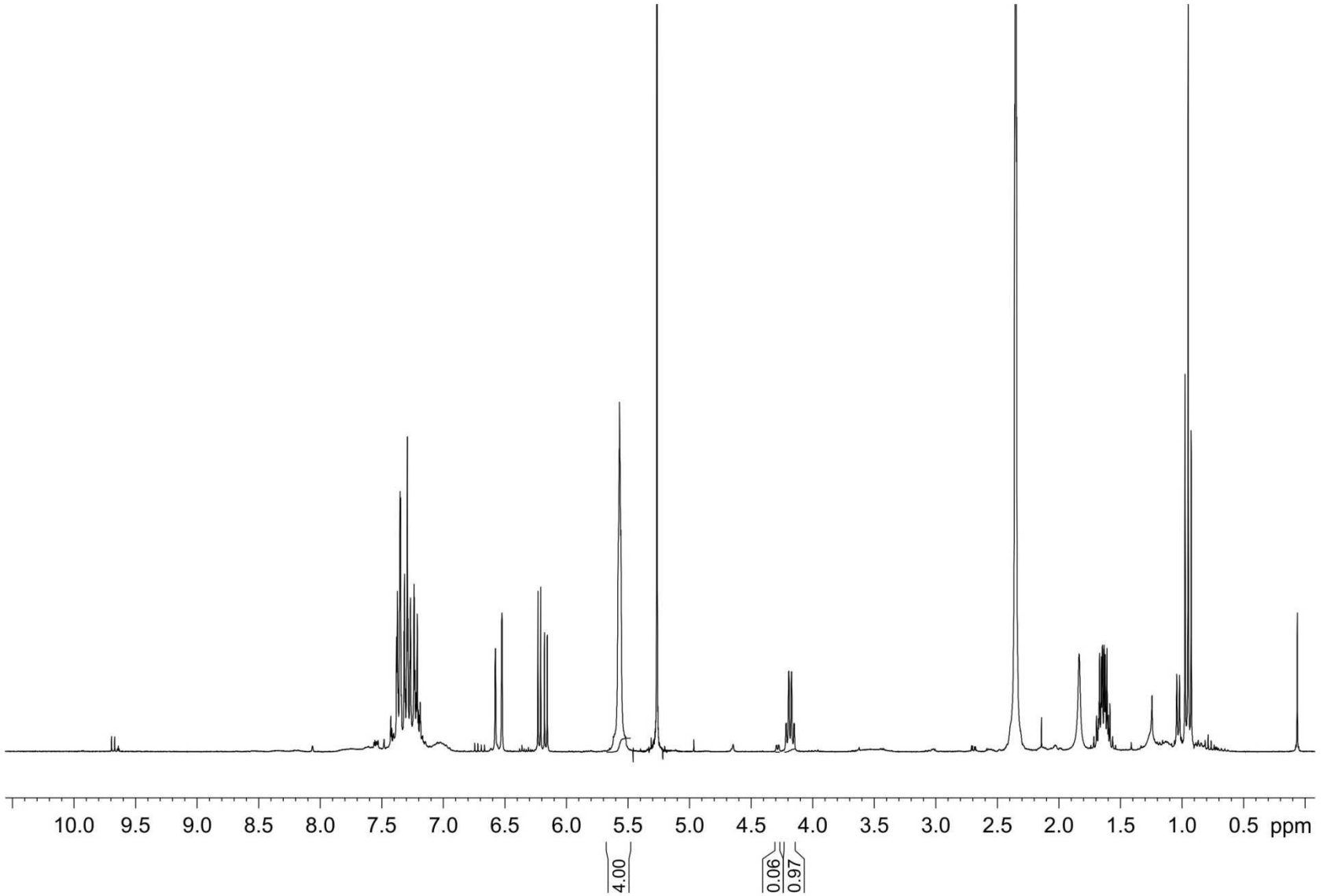

Figure S40. ^{1}H-NMR spectrum of the crude reaction mixture of the addition of Et_2Zn to cinnamaldehyde in the presence of ligand **20a** (10 mol%). Reaction time of 1.5 h. The integrals shown correspond to the internal standard (COD), (*E*)-3-phenylprop-2-en-1-ol (6%) and the adduct **22d** (97%).

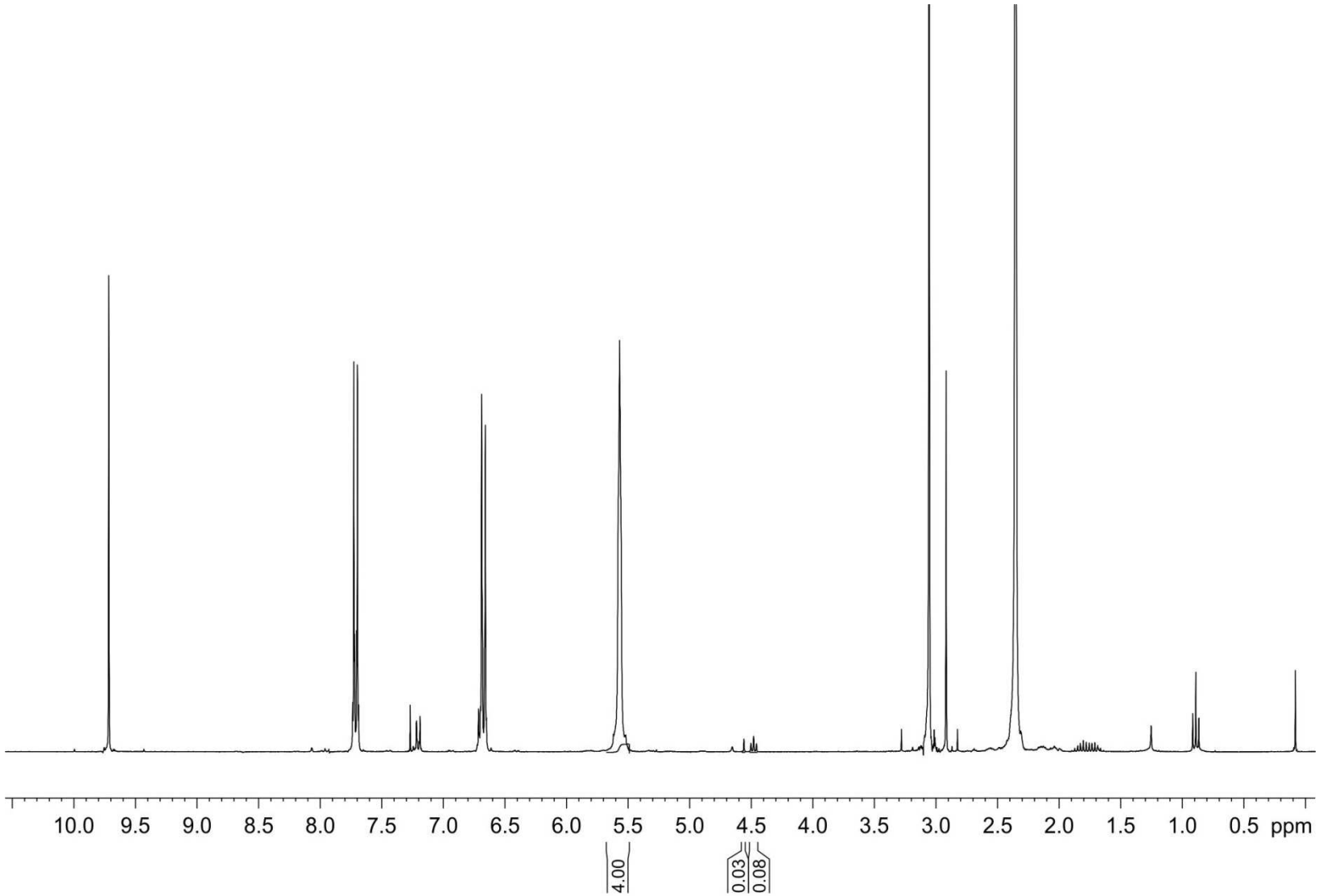

Figure S41. ^{1}H-NMR spectrum of the crude reaction mixture of the addition of Et_2Zn to 4-(dimethylamino)benzaldehyde in the absence of ligand. Reaction time of 20 h. The integrals shown correspond to the internal standard (COD), (4-(dimethylamino)phenyl)methanol (3%) and the adduct **22e** (8%).

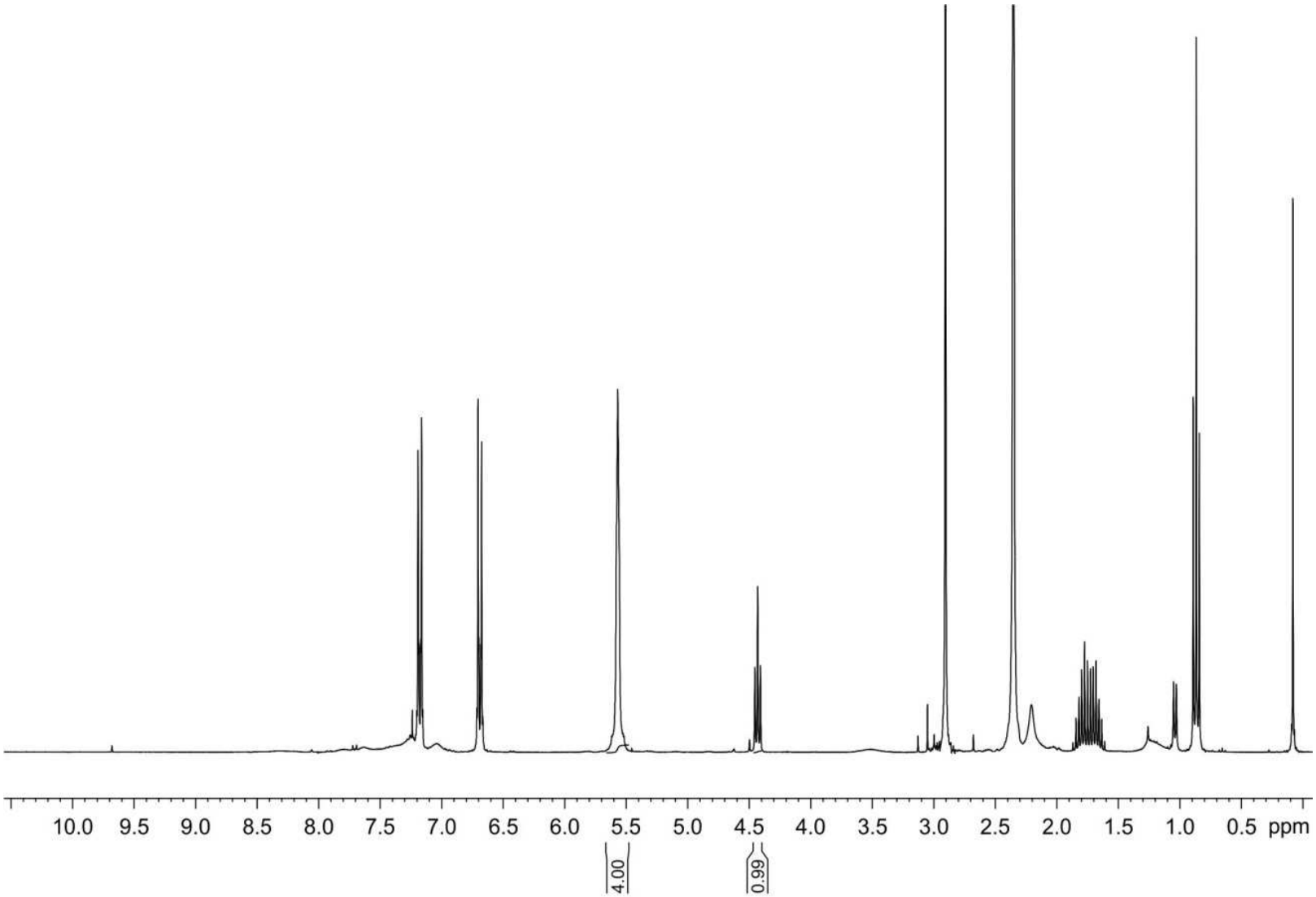

Figure S42. ^{1}H-NMR spectrum of the crude reaction mixture of the addition of Et_2Zn to 4-(dimethylamino)benzaldehyde in the presence of ligand **20a** (10 mol%). Reaction time of 20 h. The integrals shown correspond to the internal standard (COD) and the adduct **22e** (99%).

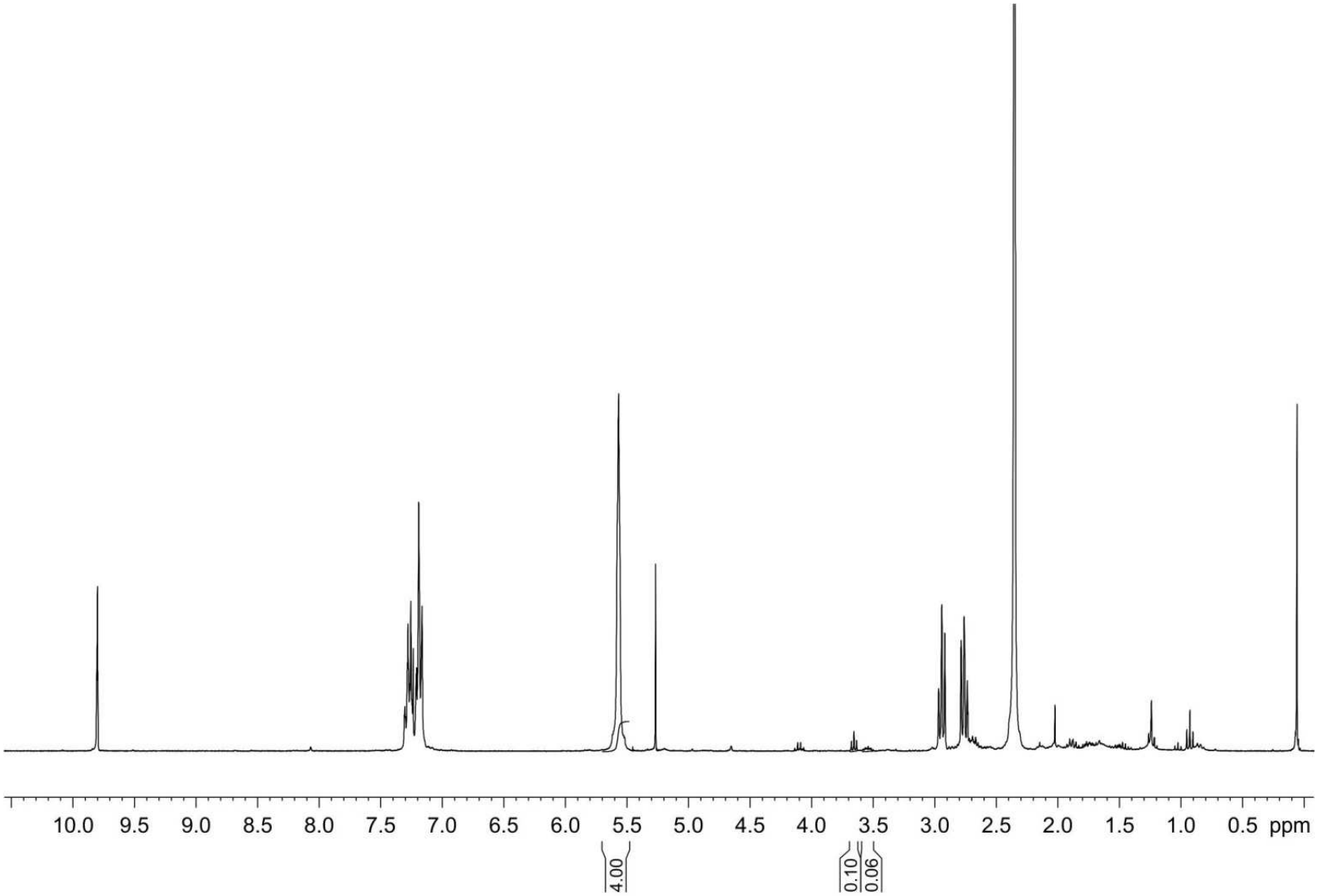

Figure S43. ^{1}H-NMR spectrum of the crude reaction mixture of the addition of Et_2Zn to hydrocinnamaldehyde in the absence of ligand. Reaction time of 4.5 h. The integrals shown correspond to the internal standard (COD), 3-phenylpropan-1-ol (10%) and adduct **22f** (6%).

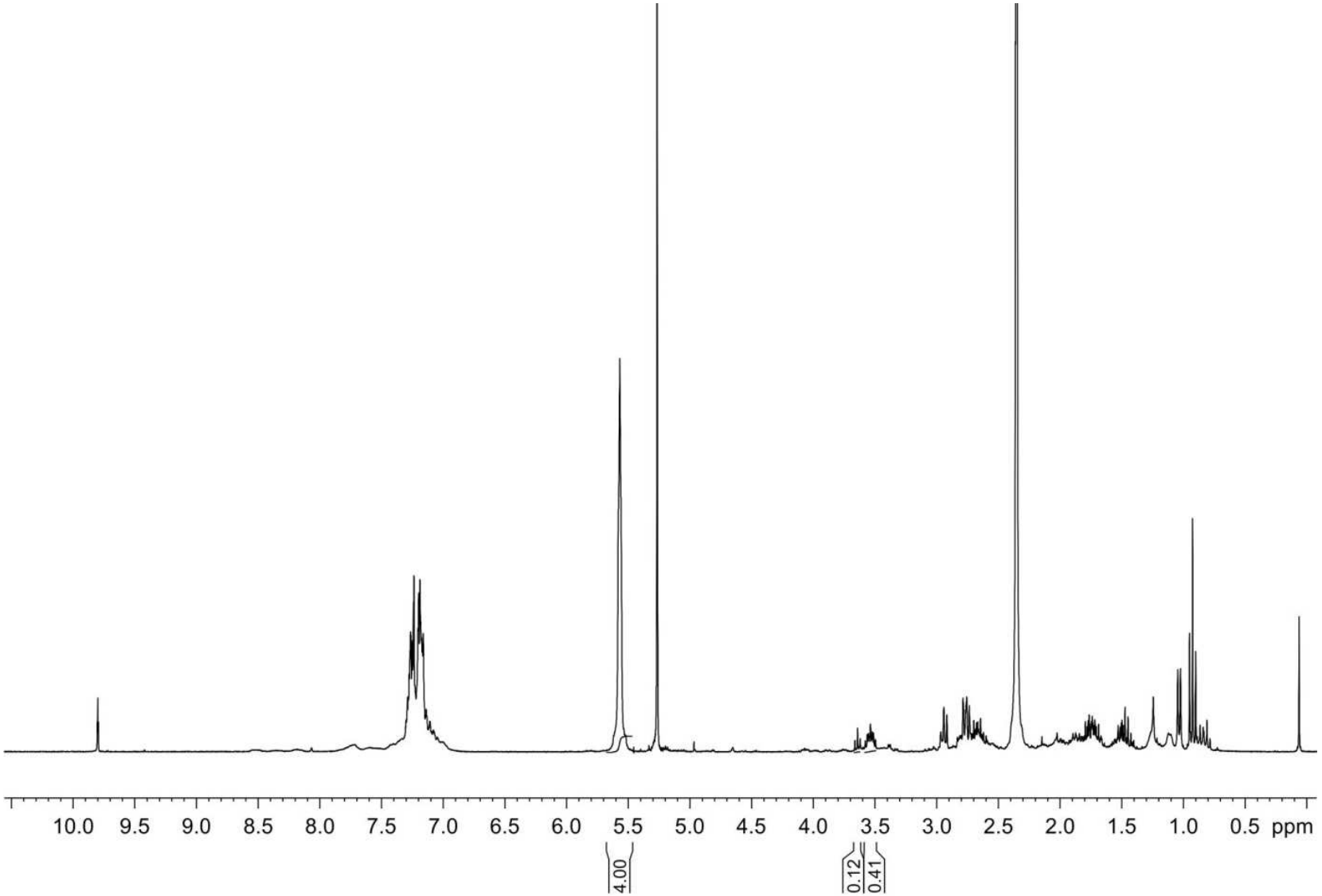

Figure S44. ^{1}H-NMR spectrum of the crude reaction mixture of the addition of Et_2Zn to hydrocinnamaldehyde in the presence of ligand **20a** (10 mol%). Reaction time of 4.5 h. The integrals shown correspond to the internal standard (COD), 3-phenylpropan-1-ol (12%) and the adduct **22f** (41%).

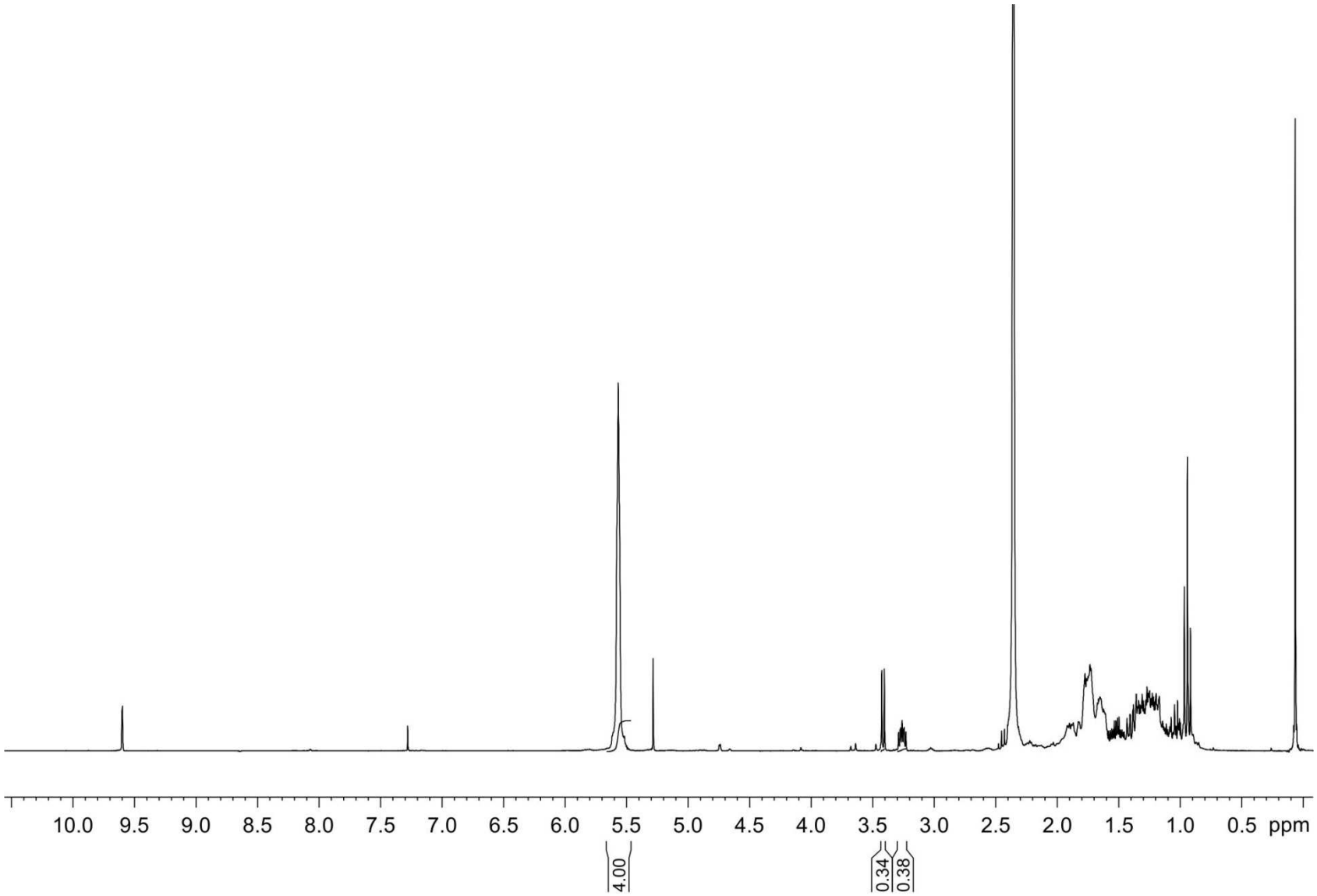

Figure S45. ^{1}H-NMR spectrum of the crude reaction mixture of the addition of Et_2Zn to cyclohexyl carboxaldehyde in the absence of ligand. Reaction time of 24 h. The integrals shown correspond to the internal standard (COD), cyclohexylmethanol (34%) and adduct **22g** (38%).

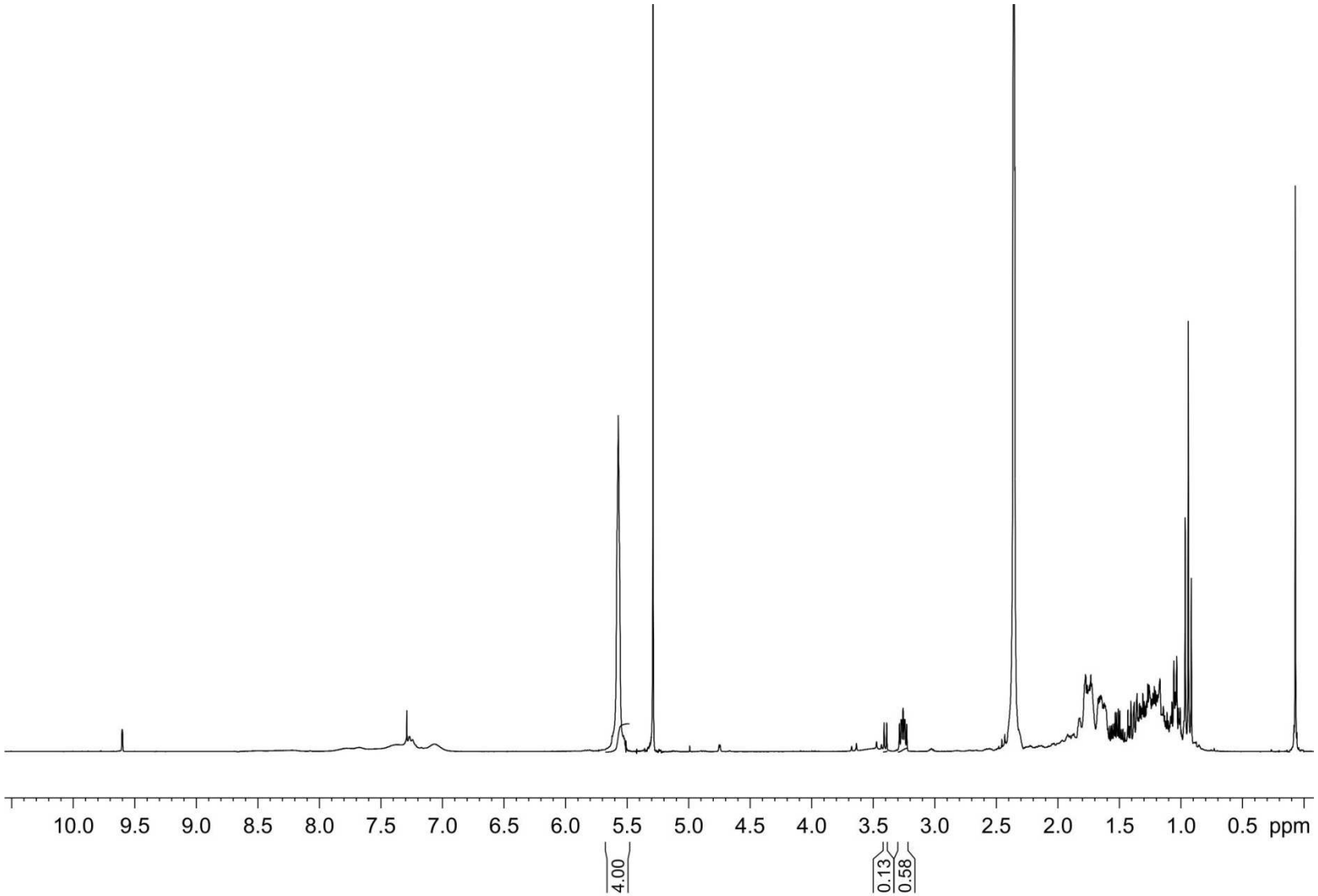

Figure S46. ^{1}H-NMR spectrum of the crude reaction mixture of the addition of Et_2Zn to cyclohexyl carboxaldehyde in the presence of ligand **20a** (10 mol%). Reaction time of 24 h. The integrals shown correspond to the internal standard (COD), cyclohexylmethanol (13%) and the adduct **22g** (58%).

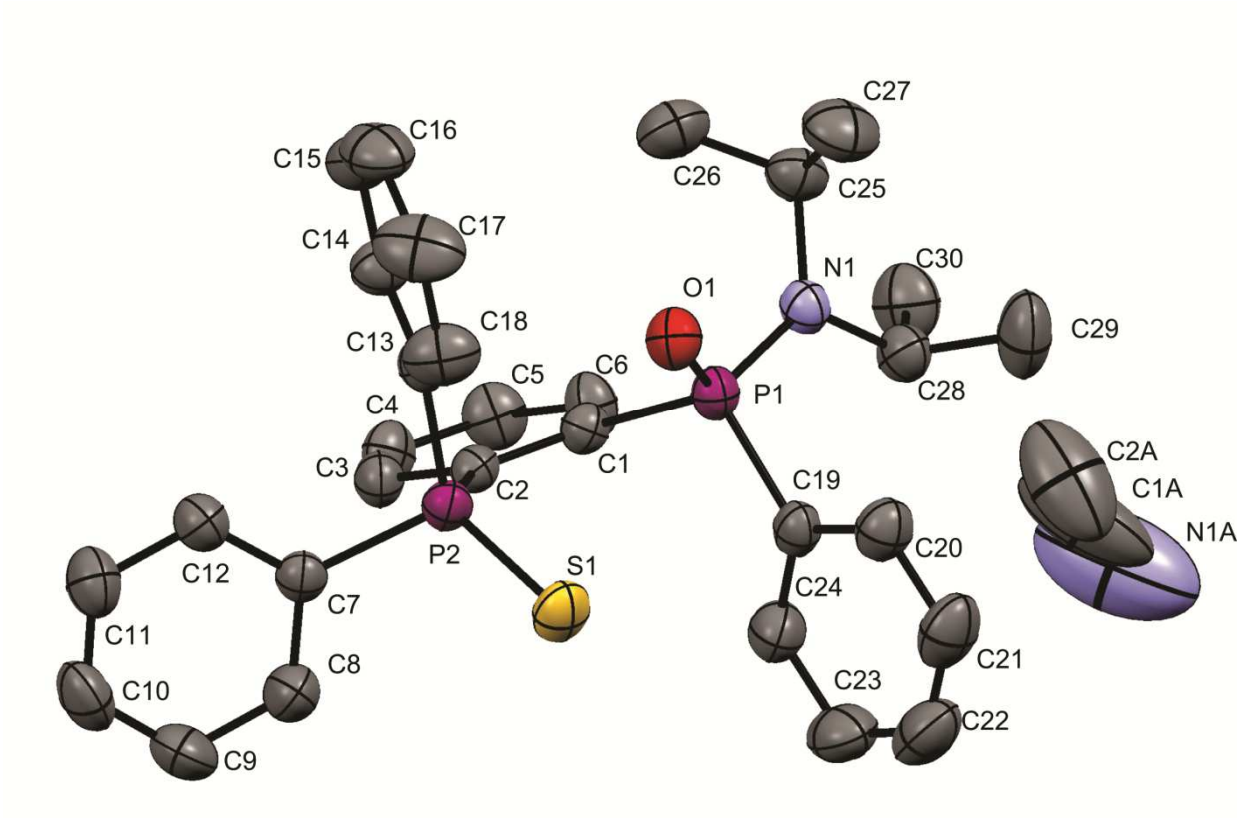

Figure S47. X-ray crystal structure of **20b** (thermal ellipsoids shown at 50% probability) including atomic numbering and solvent of crystallisation. Protons have been omitted for clarity.

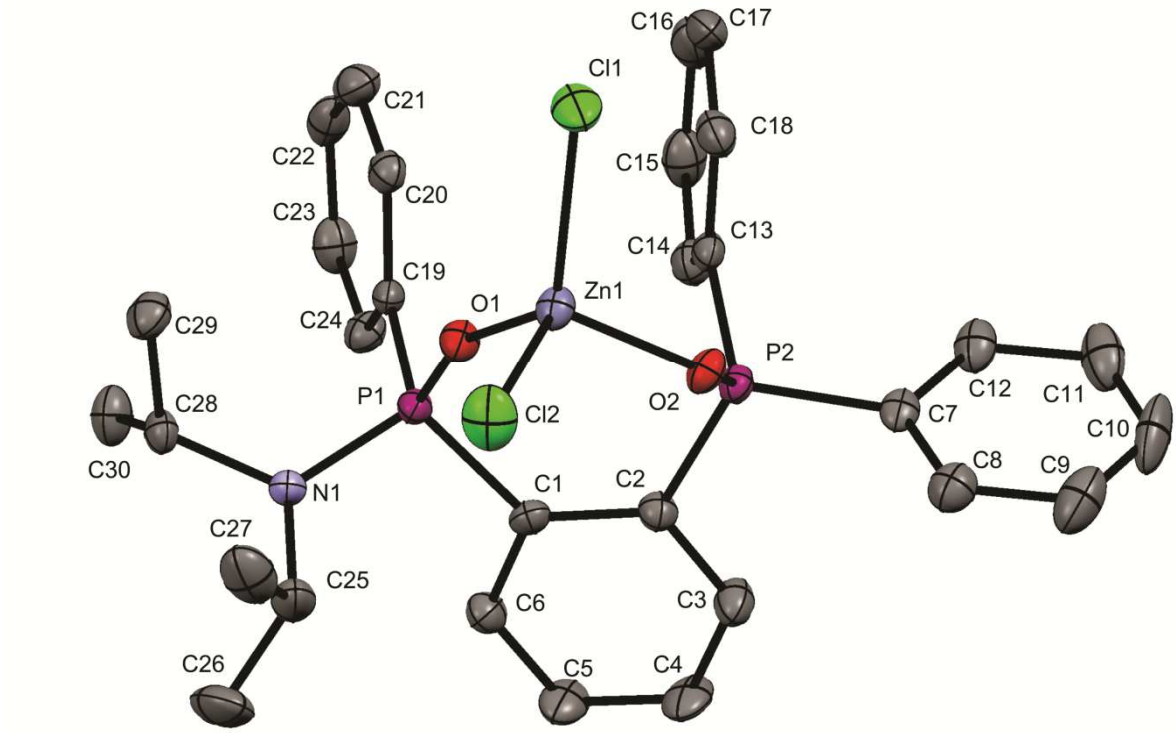

Figure S48. X-ray crystal structure of **21a** (thermal ellipsoids shown at 50% probability) including atomic numbering. Protons have been omitted for clarity.

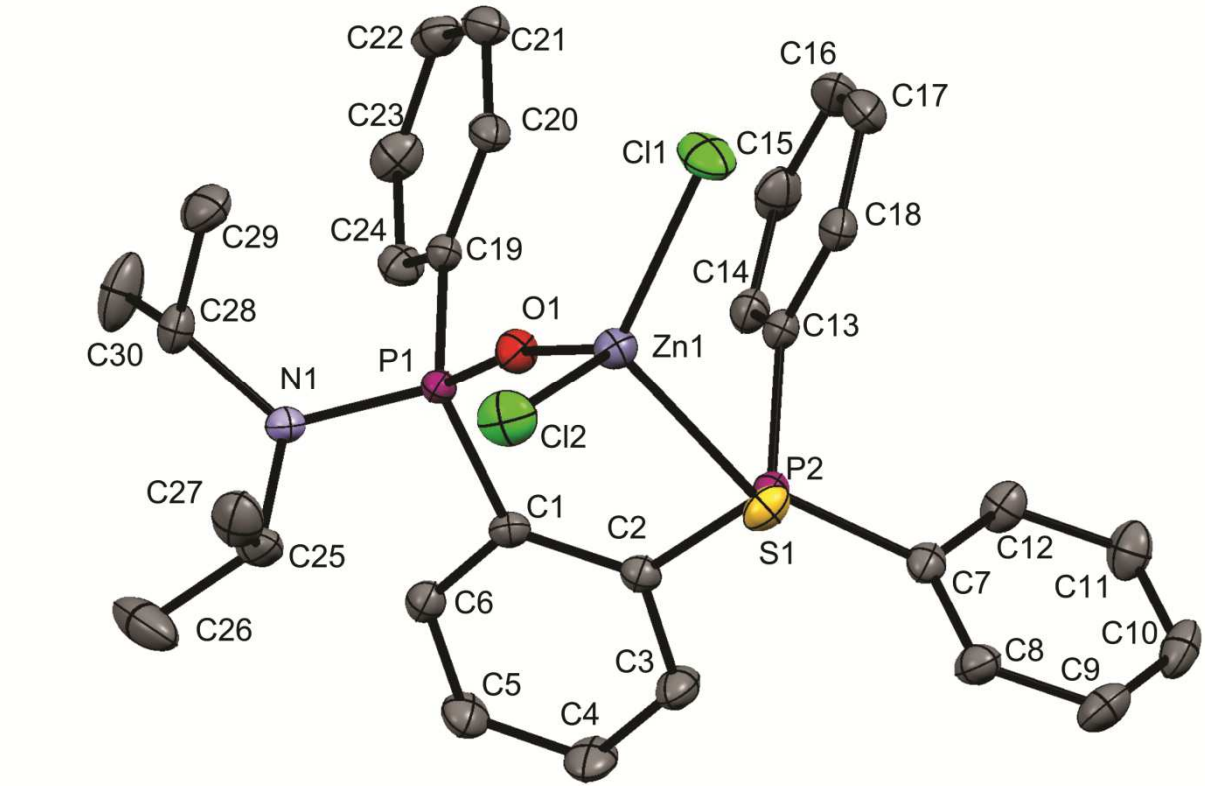

Figure S49. X-ray crystal structure of **21b** (thermal ellipsoids shown at 50% probability) including atomic numbering. Protons have been omitted for clarity.

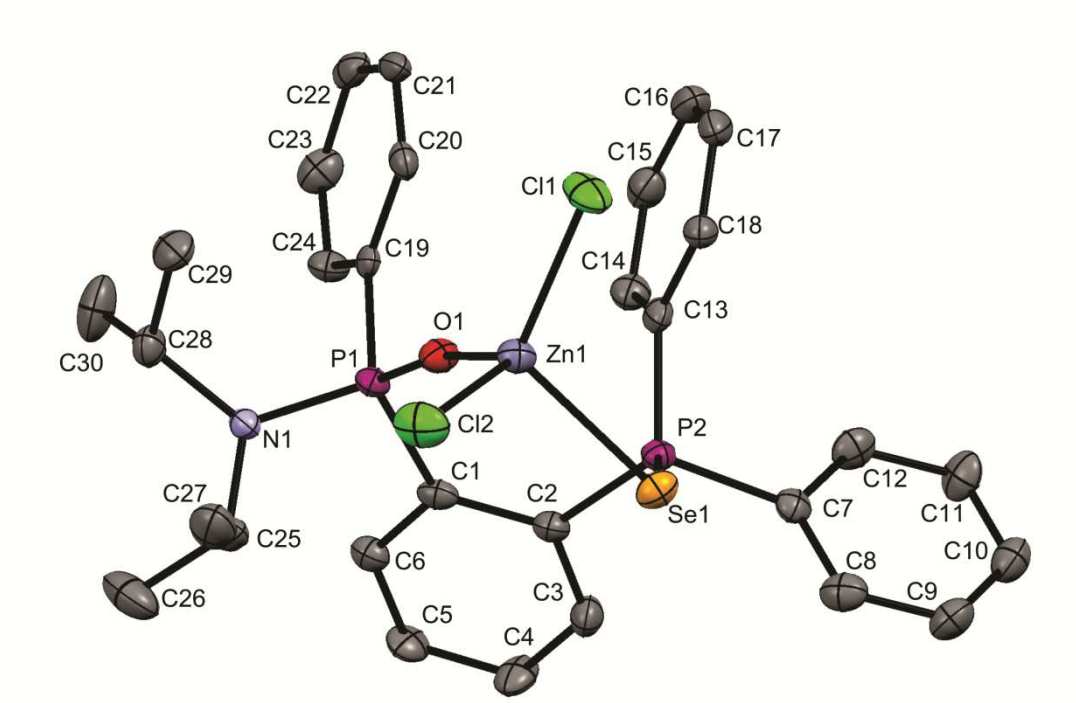

Figure S50. X-ray crystal structure of **21c** (thermal ellipsoids shown at 50% probability) including atomic numbering. Protons have been omitted for clarity.

Table S2 Selected crystal data for ligand **20b** and complexes **21a-c**

	20b	**21a**	**21b**	**21c**
Empirical formula	$C_{30}H_{33}NOP_2S\cdot C_2H_3N$	$C_{30}H_{33}Cl_2NO_2P_2Zn$	$C_{30}H_{33}Cl_2NO_2P_2SZn$	$C_{30}H_{33}Cl_2NO_2P_2SeZn$
M	558.63	637.788	653.87	700.74
Crystal system	Triclinic	Monoclinic	Monoclinic	Monoclinic
Space group	P -1	P 2_1/c	P 2_1/c	P 2_1/c
Temperature/K	293	150	150	100
a/Å	9.1412 (13),	10.7651 (4)	10.7119 (3)	10.780 (3)
b/Å	9.8502 (17),	15.5932 (5)	15.7322 (7)	15.617 (4)
c/Å	17.910 (4)	17.9816 (6)	18.1799 (7)	18.356 (5)
α(°)	93.263 (18)			
β(°)	94.429 (17)	91.666 (3)	93.429 (3)	93.696 (7)
γ(°)	109.92 (2)			
V/Å ^{3}	1505.6 (5)	3017.16 (18)	3058.2 (2)	3083.9 (14)
Z	2	4	4	4
μ/mm^{-1}	0.24	1.13	1.18	2.28
D_{calcd}/g cm^{-3}	1.232	1.404	1.420	1.509
Crystal dimensions/mm	0.21 × 0.13 × 0.10	0.13 × 0.09 × 0.05	0.42 × 0.34 × 0.13	0.31 × 0.07 × 0.05
F(000)	592.0	1320.0	1352.0	1424.0
θ range for data collection/°	3.52-25.35	1.89-25.35	1.91-25.35	1.71-25.05
Refls. measured	10485	12064	16631	16631
Refls. unique	5486	5516	5446	5572
Parameters/restraints	344	343	343	343
GOF on F^2	0.93	1.11	1.15	1.06
*R*1 [$I \geq 2\sigma(I)$]	0.048	0.046	0.031	0.053
*wR*2 (all data)	0.112	0.137	0.090	0.0109
$\Delta\rho_{max}/\Delta\rho_{min}$/e·Å $^{-3}$	0.32, −0.30	0.63, −0.71	0.47, −0.51	0.70, −0.54

Table S3 Selected bond lengths (Å) and angles (°) for complexes **21a-c**

21a		**21b**		**21c**	
P1-O1	1.496(3)	P1-O1	1.495(2)	P1-O1	1.497(3)
P1-N1	1.647(3)	P1-N1	1.641(2)	P1-N1	1.647(4)
P1-C1	1.831(4)	P1-C1	1.833(2)	P1-C1	1.833(4)
P1-C19	1.792(4)	P1-C19	1.796(2)	P1-C19	1.798(5)
P2-O2	1.504(3)	P2-S1	1.9987(9)	P2-Se1	2.158(1)
P2-C2	1.832(4)	P2-C2	1.828(2)	P2-C2	1.833(4)
P2-C7	1.801(3)	P2-C7	1.821(3)	P2-C7	1.831(5)
P2-C13	1.794(4)	P2-C13	1.799(2)	P2-C13	1.793(5)
Zn1-O1	1.972(3)	Zn1-O1	1.967(2)	Zn1-O1	1.975(3)
Zn1-O2	1.977(2)	Zn1-S1	2.3620(7)	Zn1-Se1	2.4638(9)
Zn1-Cl1	2.215(1)	Zn1-Cl1	2.2188(7)	Zn1-Cl1	2.224(1)
Zn1-Cl2	2.202(1)	Zn1-Cl2	2.2220(8)	Zn1-Cl2	2.230(2)
Zn1-O1-P1	159.1(2)	Zn1-O1-P1	166.4(1)	Zn1-O1-P1	166.6(2)
Zn1-O2-P2	129.9(1)	Zn1-S1-P2	104.21(3)	Zn1-Se1-P2	99.88(4)
O2-Zn1-O1	90.4(1)	S1-Zn1-O1	94.29(5)	O1-Zn1-Se1	93.83(9)
Cl1-Zn1-Cl2	114.89(5)	Cl1-Zn1-Cl2	110.96(3)	Cl1-Zn1-Cl2	110.47(6)
Cl2-Zn1-O2	114.92(8)	Cl2-Zn1-S1	109.68(3)	Cl2-Zn1-Se1	109.85(4)
O1-P1-C1-C2	-23.5(4)	O1-P1-C1-C2	-22.1(2)	O1-P1-C1-C2	-21.9(4)
P1-C1-C2-P2	-5.9(5)	P1-C1-C2-P2	-5.1(3)	P1-C1-C2-P2	-4.7(6)
O2-P2-C2-C1	68.3(4)	S1-P2-C2-C1	77.5(2)	Se1-P2-C2-C1	78.7(4)
C1-P1-O1-Zn1	-22.8(5)	C1-P1-O1-Zn1	-48.3(5)	C1-P1-O1-Zn1	-64.9(9)

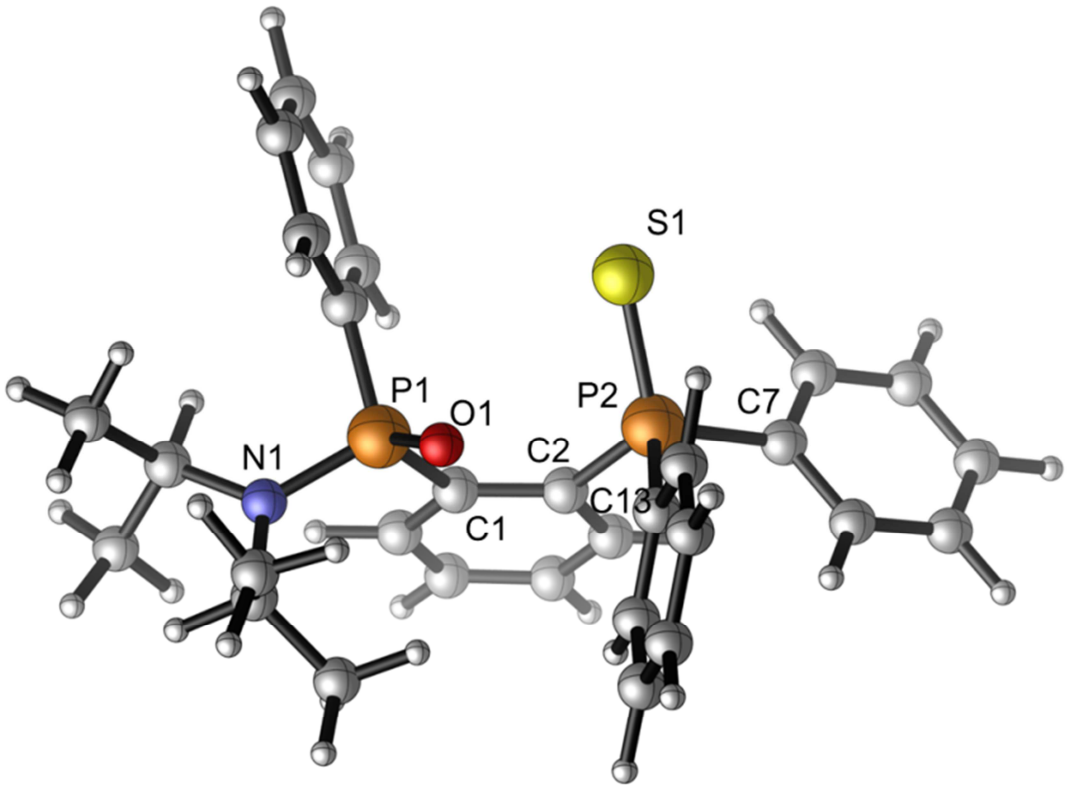

Figure S51. Calculated molecular structure of **20b**. The same numbering scheme as for the X-ray diffraction single crystal structure was used.

Table S4. Cartesian coordinates (Å) for the optimized structure **20b**.

0 1

P	-1.86281600	-0.34407600	0.45222600
P	1.58584700	0.12389300	0.11441800
S	-1.21937100	-1.58243400	1.85106600
O	0.86006500	0.98702200	1.09374500
C	4.18922600	0.17899200	-0.87401000
H	3.96896700	-0.88925400	-0.83450300
N	2.92892200	0.87966200	-0.54174700
C	-0.94465200	-0.47670000	-1.15208000
C	0.45744100	-0.34999000	-1.26669700
C	-3.60264800	-0.74168200	0.01117500
C	-4.55627500	0.25059400	-0.21999400
H	-4.29538000	1.29851200	-0.13287500
C	-1.07281800	-0.99291800	-3.52786100
H	-1.67867800	-1.23168000	-4.39435100
C	-1.92464000	3.74538200	0.21748900
H	-1.85576600	4.50015000	-0.55796300
C	-1.68813700	-0.78303000	-2.29646400
H	-2.76594900	-0.86488200	-2.24149300
C	1.05305700	-0.57378000	-2.50768100
H	2.12854200	-0.48369400	-2.59619400

C	-1.91873900	1.42772600	0.87707700
C	0.30539400	-0.90197200	-3.63420600
H	0.80014200	-1.07427500	-4.58307700
C	-6.21825900	-1.44055900	-0.67191400
H	-7.23475600	-1.71171600	-0.93404700
C	2.06224100	-2.67331300	0.16953000
H	1.55417900	-2.74296500	-0.78618700
C	-1.84772500	2.39821000	-0.12135100
H	-1.71938000	2.10991300	-1.16017800
C	-2.07720300	4.12106500	1.54925300
H	-2.12911600	5.17146300	1.81294900
C	2.21257200	-1.43941200	0.80095200
C	-5.86185100	-0.10215400	-0.55716700
H	-6.59939500	0.67448100	-0.72439200
C	-5.26838700	-2.43375200	-0.43998600
H	-5.54218700	-3.47948500	-0.52023000
C	2.83859800	-1.36753200	2.04693900
H	2.92826600	-0.40947800	2.54997700
C	-3.96909500	-2.08684800	-0.09261200
H	-3.23428800	-2.85988000	0.10429400
C	3.18487500	-3.75189200	2.01148900
H	3.56108400	-4.65283000	2.48283200
C	2.93063000	2.35871000	-0.67150400
H	3.84242900	2.59243100	-1.22416800
C	3.32564300	-2.52175300	2.64975300
H	3.80595600	-2.46247600	3.61973000
C	4.69492100	0.48634100	-2.28883700
H	3.89829100	0.44762600	-3.03410100
H	5.16658600	1.47008500	-2.35030100
H	5.45385000	-0.25052500	-2.56346600
C	1.75139400	2.85672100	-1.50506200
H	1.73045900	2.37366800	-2.48528600
H	0.80526800	2.65895400	-0.99339400
H	1.83033900	3.93738600	-1.65185200
C	5.28867800	0.47765700	0.14503300
H	4.97516300	0.20765400	1.15535100
H	6.19201200	-0.08779800	-0.10033300
H	5.54640800	1.54094200	0.13263100
C	2.55139600	-3.82710500	0.77464200
H	2.42926700	-4.78592800	0.28387400
C	-2.07696900	1.80050200	2.20853000
H	-2.11217500	1.03979900	2.98089500
C	-2.15756200	3.14847400	2.54223300
H	-2.27062400	3.43921600	3.58031500
C	3.00762400	3.09099600	0.67096800
H	3.79299100	2.66780800	1.30100900
H	3.23616700	4.14698000	0.49901600
H	2.06044600	3.01579200	1.20524800